EXAMENSARBETE

Adaptive clutter suppression in airborne surveillance radar

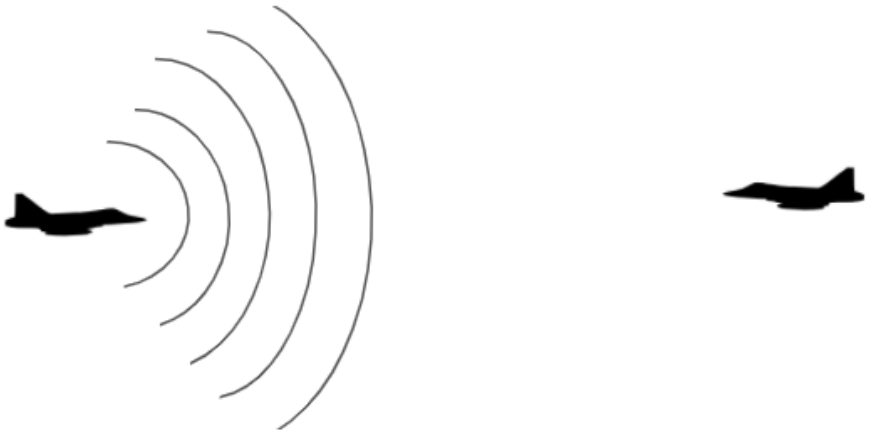

Sabina Björk

Rymdteknik, master
2021

Luleå tekniska universitet
Institutionen för system- och rymdteknik

LULEÅ TEKNISKA UNIVERSITET

Adaptive clutter suppression in airborne surveillance radar

Author
Sabina Björk

Supervisor
Björn Hallberg,
SAAB Surveillance

Examinator
Jaap van de Beek,
Luleå University of Technology

August 2021

Abstract

Air- and spaceborne radars play an important role for civilian and military use. There are numerous applications such as earth observations, surveillance and others. High performance clutter suppression is a crucial part of many of these radar systems. *Space time adaptive processing*(STAP) has become a topic of interest for clutter suppression applications. Although for most *moving target indication*(MTI) radars other applications are used for clutter suppression. This master thesis analyses STAP on two antenna configuration for airborne radar applications. The first configuration based on auxiliary antennas, the second configuration based on a multitapering method called *discrete prolate spheroidal sequences(DPSS)*. This theses shows that both antenna configurations are valid choices for STAP applications. Although the later configuration, DPSS, has a higher clutter suppression performance in general. However, one problem with the DPSS configuration seems to be there are fundamental limitations with the configuration. These limitations are shortly discussed in this theses but more work should be done before implementing the DPSS configuration.

Sammanfattning

Flygburna radarsystem har en viktig roll för både civila och militära bruk, som bland annat jordobservationer, övervackning med mera. För många av dessa radarsystem är en hög prestanda för klotterundertryckning mycket viktigt. Space-time adaprve processing(STAP) är en intressant metod för adaptiv klotterundertryckning. Traditionell används andra metoder för klotterundertryckning. Detta examensarbete appliserar STAP och jämför två antennkonfigurationer. Den första konfigurationen använder så kallade hjälpkanaler(hjälpantenner). Den andra konfigurationen använder en multitaperande metod så kallad *discrete prolate spheroidal sequences(DPSS)*. Resultatet av detta examensarbete visar att DPSS konfigurationen generellt presterar bättre. Dock finns problem med DPSS konfigurationen som undantagsvis misslyckas med undertryckningen av klotter. Detta diskuteras kort i rapproten.

Acknowledgment

I would like to thank Saab Surveillance for the opportunity to write this thesis. I am thankful for all the support and helpful comments from the whole team. I would like to express my sincere gratitude to my supervisor Björn Hallberg. His guidance, feedback and help has been very appreciated. I would also like to thank my manager Ninva Shamoun who, and Björn Hallberg, believing in me.

Also I would like thank my friends at the university who has been by lab partners, study buddies and friends through all these years. Extra thanks to Niklas and Erik, without them my time at the university would not have been the same.

Last but not least, I would like to thank my family for supporting and believing in me.

In memory of Johan Andersson

(1957-11-15 - 2021-04-04)

Rest in peace.

Contents

Abbreviations

Abbreviation	Meaning
AESA	Active Electronically Steered Array Antenna
ESA	Electronically Steered Array Antenna
DF	Doppler filtering
PC	Pulse compression
PRF	Pulse Repetition Frequency
PRI	Pulse Repetition Interval
SLC	Sidelobe Cancellation
STAP	Space Time Adaptive Processing

Operators

Notation	Meaning
$\overline{A}$	Complex conjugate of elements in matrix A
A^T	Transpose of matrix A
A^H	Hermitian transpose, the same as $\overline{A}^T$
EA	The expected value of A
tr(A)	The trace of A

Varibles

Notation	Meaning
N	Number of antenna elements
Q	Covariance matrix
T	Transformation matrix
IF	Improvment factor
CNR	Clutter to Noise ratio
SINR	Signal to Interferance and Noise ratio

Chapter 1

Introduction

Radar transmit signals to get information about the surroundings by analysing the signals reflected back from the surroundings. From the reflected signals the radar can determine the location and movement of objects in the direction of the transmitted signals. For surveillance radars the reflected signals of interest are mostly signals reflected of other aircraft's or possible threats in the air. The objects of interest are usually called targets. How the radar determines the location of targets will be described in chapter 2. Determination of the movements of targets are done by analysing the Doppler effect. Due to the Doppler effect the moving targets will have a Doppler velocity relative to the radar, which will indicate which direction the targets are moving. More about the Doppler effect can be found in chapter 2. However, the radar will not only detect signals reflected of the target but also other reflected signals, unwanted signals. These unwanted signals are called clutter signals, which are interference in the radars received signal. For an airborne surveillance radar the clutter mostly consist of ground echos, which are signals reflected from the ground. These ground echos interferes with the reflected signals of the target and the radar need to process these signals to be able to distinguish the target from the clutter.

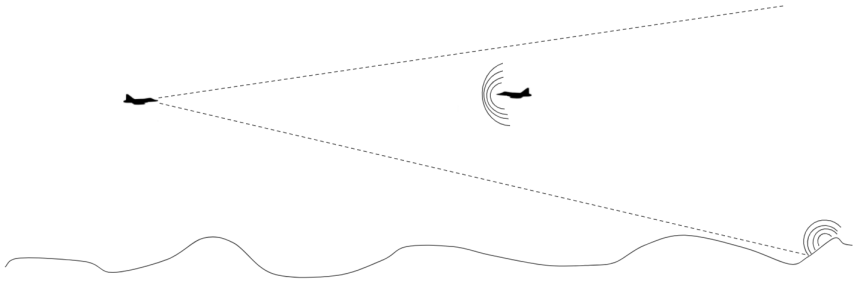

Figure 1.1: Illustration of radiated signal from the radar reflected by target and the ground.

These ground echos will, like the target, have a Doppler velocity relative the radar. The targets Doppler velocity will for most cases be much greater than the Doppler velocities of the ground

echos which makes it easy to distinguish the target from the ground echos. Although, for some parts of the ground the Doppler velocity of the ground echos relative to the radar will be close to or equal to the targets Doppler velocity relative to the radar. For these cases it is harder to detect the targets Doppler velocity. That is why high performance clutter suppression is important for an airborne surveillance radar to be able to detect target signals over a background of high clutter returns. Clutter suppression are methods for reducing the unwanted clutter in the received signal. There are a couple of different ways to suppress clutter. In this thesis *Space Time Adaptive Processing(STAP)* is analysed for clutter suppression.

STAP is a clutter suppression method applicable on *electronically steered array antennas*(ESA), illustrated in figure (1.2) . Which has an array of antenna elements, where each antenna element is a separate antenna. Thus, the ESA receives as many signals as there are antenna elements. Traditionally, these signals are added up and then processed as one signal. More information about how an ESA works can be found in chapter 2.1.1. However, an ESA allows multi-channel processing of the incoming signals. Thus, one can process the incoming signals in several channels and compare the different processing for optimal results.

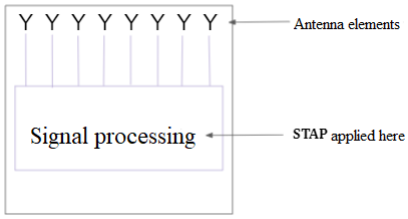

Figure 1.2: A basic illustration of an ESA antenna with an array of antenna elements.

In this thesis two different antenna configurations using STAP are compared and analysed. Both configurations are ESA antennas. The difference between the two configurations are the multi-channel processing methods.

1.1 Problem

In signal processing one often weights the incoming signals, which is done by multiplying the amplitudes of the signal to a desired value. This is called tapering. There are several methods for tapering. Usually high amplitudes are desirable in the direction of the target, while in other directions one wants lower amplitudes. See figure 1.3 , here the vertical axis represents the amplitude of an incoming signal and the horizontal signal represents the distance along the aperture of the radar(along the antenna elements). In the figure there are two signals illustrated, one tapered and one untapered. Here the tapared signal has focused the amplitude of the incoming signal in the direction in the middle. This is translated to the target is located straight ahead of the radar. At the ends of the radar mostly clutter will be received, which is not of interest thus one decreases the amplitudes.

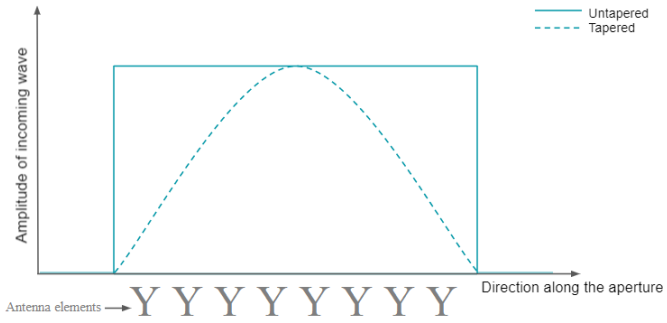

Figure 1.3: Basic illustration of a tapered and untapered received signal. The amplitudes of the tapared signal has been weighted to maximize the amplitude in the direction of the target and lower the ampitudes in other directions.

In radar theory, the incoming signals of radars are often illustrated in so called antenna diagrams instead as shown in figure 1.4. Here the vertical axis shows the normalized gain of the antenna and the horizontal axis represents the normalized angle of the signal. Again, there is a tapered and an untapered signal illustrated. In this figure one can identify one large lobe so called the *mainlobe*, and several smaller lobes so called *sidelobes*.

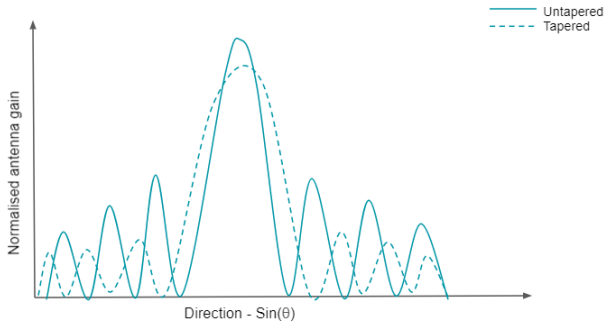

Figure 1.4: Illustration of an antenna diagram of received signal, both tapered and untapered

The methods traditionally used for clutter suppression includes decreasing the sidelobes in the antenna diagram by tapering,as illustrated in figure 1.4. When decreasing the sidelobes most methods usually also decreases the mainlobe, this is a problem. Since there are physical limitations of the hardware one can not always afford a power loss in the mainlobe. For an optimal method of clutter suppression there should be no power loss in the mainlobe.

Thus, the problem with traditional clutter suppression methods is the power loss in the mainlobe of the antenna diagram when decreasing the sidelobes, especially when the clutter directions are close to the mainlobe. In theory the power loss in the mainlobe should be avoided when using STAP for clutter suppression.

1.1.1 Antenna configuration 1 - auxiliary antennas

The first antenna configuration for clutter suppression relies on using auxiliary antennas. Auxiliary antennas are separate antennas, which can be used as reference antennas(help antennas). Since the main antenna for this thesis is an ESA with several separate antenna elements as shown in figure 1.2, one can choose antenna elements to be auxiliary antennas. Thus no extra antennas are needed. By comparing the incoming signals from the main antenna(all antenna elements) to the auxiliary antennas one can define the angles and magnitude of the clutter signals. Applying STAP to the signals results in an optimal weighting which cancels out the clutter signals, while maximising the mainlobe.

Figure 1.5 shows a basic illustration of a received signal for the case when three channels are used for antenna configuration 1. In the figure to the left the first channel may look familiar, compare to figure 1.3. Note that channel one is tapered. Here the first channel contains data from all antenna elements. While the auxiliary channels(help channels) only contain data from chosen auxiliary antennas, in the auxiliary channels all other antenna elements are zeroed. As mentioned earlier, in radar theory one usually illustrates the incoming signals in antenna diagrams. In figure 1.5 to the right an antenna diagram for configuration 1 is shown. Again, the first channel looks familiar, the two auxiliary channels only consist of one wide mainlobe. However, the figure illustrated three channels and these channels are compared to find the optimal weight for clutter suppression.

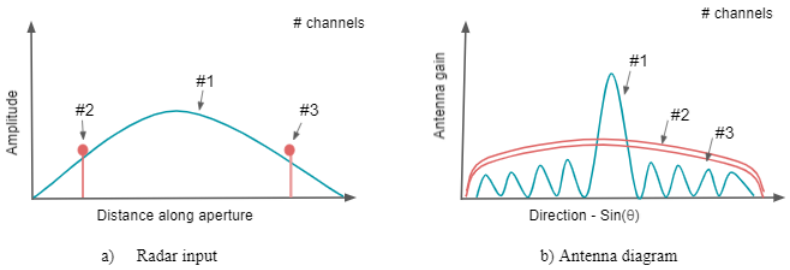

Figure 1.5: Basic illustrations of the received signals of antenna configuration 1

More about antenna configuration 1 is found in chapter 3.1.

1.1.2 Antenna configuration 2 - discrete prolate spheroidal sequence

The second antenna configuration for clutter suppression uses so called *discrete prolate spheroidal sequences(DPSS)*, which is a method for multitapering. Here the incoming signals are taperd in more than one way. These taperings are compared and clutter angles and magnitudes can be detected. Applying STAP on the taperings results in optimal weighting which minimizes the clutter amplitudes while preserving the power in the mainlobe.

Figure 1.6 shows a basic illustration of a received signal for the case when three channels are used for antenna configuration 2. Again, the first channel in the figure to the left looks familiar, compare to fig 1.3. The first channel contain data from all antenna elements and is tapered in one way.

The other channels also contains data from all antenna elements. However, the other channels are tapered in different ways. In other words the channels have different weights for the incoming signal. The antenna diagram of configuration 2 is illustrated to the right in figure 1.6. Here there are three channels that contains data from all antenna elements, these channels are compared to to maximise the mainlobe and minimize clutter.

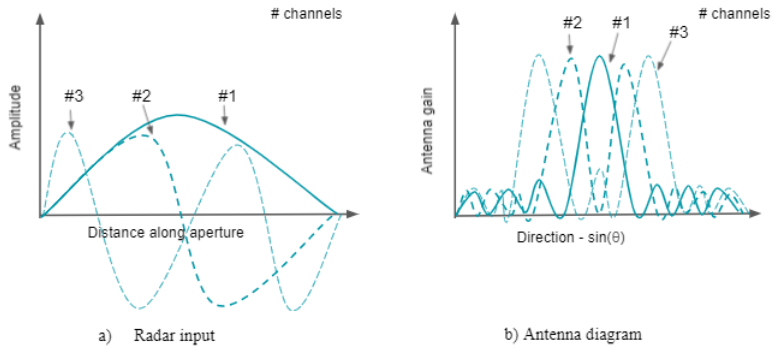

Figure 1.6: Basic illustration of the received signals of antenna configuration 2

More about antenna configuration 2 is found in chapter 3.2.

1.2 Purpose

The purpose of this master thesis is to compare two different antenna configurations using STAP for clutter suppression for airborne radar systems. The antennas for the configurations are the same. However, the signal processing of the incoming signals will differ for the two configurations. By using STAP on these configurations one can suppress clutter signals without a power loss in the mainlobe. In STAP, the statics of the clutter in space and time domain are estimated from radar training data and described by a covariance matrix. The covariance matrix contains the relation between clutter and noise. A space-time filter is subsequently applied by aid of the coveriance matrix and a model of signal data, in order to maximize signal energy while minimizing clutter energy. Thus, the purpose of this thesis is to compare these two antenna configurations by analysing which configuration generate the best estimated $\mathbf{Q}$ using the smallest training data set while cancelling clutter signals and maximizing the mainlobe.

1.3 Limitations

Basic models for the antenna configurations are used for simulations. Only the sidelobe cancellation(clutter suppression) part of signal processing is modelled. The incoming signal is simulated with noise assumed to be white Gaussian noise and clutter assumed to be Gaussian noise. All simulations are made with only one target, located in the mainlobe.

Chapter 2

Theory

Some refreshment of basic radar theory, signal processing and signal processing for radar supplications can be good to get a better understanding of how and why these two antenna configurations are interesting. There are much more that can be said about radars and signal processing, however this chapter covers what is needed to get an understanding of the results in this thesis.

2.1 Basic Radar Theory

Radars are used to detect objects, such as vehicles, airplanes, satellites etc. By sending radio waves the radar can detect objects when the waves are reflected by the surroundings. The radar can by "listening" to the echos "see" the objects. Since the atmosphere is almost completely transparent one can use radars to not only "see" objects in the night as well as in the daylight, but also through clouds and fog. Compare to visual light that are absorbed by the clouds. To do this the radar needs a transmitter to tramsmitt the waves, a receiver to receive the echos, and antennas. Usually the transmitter and receiver share a common antenna. A basic single antenna model is illustrated in figure 2.1. There are many different antennas that can be controlled and steered in different ways [12].

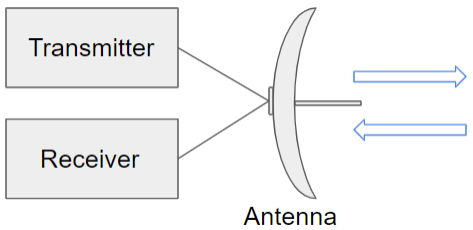

Figure 2.1: A Basic Signal Antenna Model

It is not satisfactorily to only detect the object, more information about the target is desirable. The target is the object of interest. Once a target is found, how does one know where it is located or

where it is headed? Let's start with describing how to determine the range (distance) to the target. It can be determined by measuring the time it takes from one transmitted pulse to be reflected and received. The range becomes:

$$R = \frac{c\tau}{2} \tag{2.1}$$

Here c is the speed of light and τ is the time between the transmitted and received signal. Since τ is the time it took the signal to get to the target and back one gets twice the distance between the radar and the target, thus in equation (2.1) the expression is divided by two[12].

To avoid problem with transmitting and receiving at the same time, one usually sends pulses and turn off the receiver during transmission. The rate that the pulses are transmitted is called *Pulse Repetition Frequency (PRF)*. In between transmission the receiver is back on. The result of this is illustrated in figure 2.2. Note that it takes time for the pulses to be reflected and received. The figure illustrates an example where the radar has time to transmit three pulses before it receives the first echo. The time interval between two transmitted signals is called the *Pulse Repetition Interval (PRI)*[12].

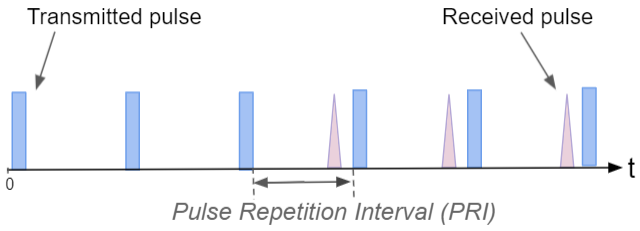

Figure 2.2: Transmitted and received pulses

The problem now is, how does one know which transmitted pulse the received signal came from? In figure 2.2, the first echo could come from pulse no. 1, 2 or 3. If echos are paired with the wrong pulse, then the time used in equation (2.1) will be incorrect. Thus, the calculation will generate false results for the range of the target. This is not acceptable for a radar. The radar needs to be able to identify which pulse the echo came from. To determine this one changes the PRF and transmits new pulses, and uses the fact that time is inversely proportional to frequency. Results in a set of *Pulse Repetition Interval (PRI)*.

$$PRI = \frac{1}{PRF}$$

Doing this will result in a set of possible ranges for the target. One of these ranges from the second PRF is the same as for the first PRF. This range becomes the hypothesis, one confirms the hypothesis by testing with a third PRF. If the hypothesis range is a match with one of the ranges in the third possible range set, the radar will conclude that the hypothesis is true. Thus, the radar

now knows the range of the target. [12] A basic example of this is shown in figure 2.3, where a range of 18000 m if found for each PRF. Thus, the range of the target has to be 18000 m.

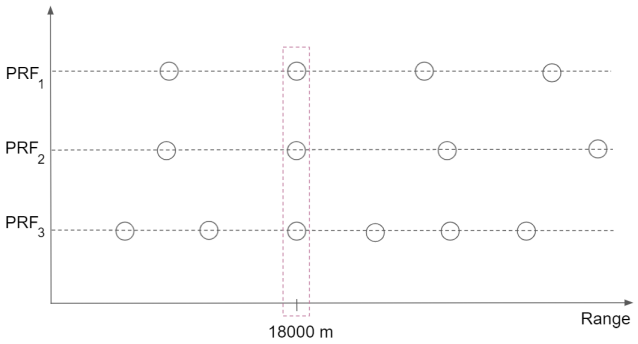

Figure 2.3: Illustration of varying the PRF to identify the range to the target.

But how does the radar determine where the moving target is heading? Using the Doppler effect, the radar can calculate the Doppler velocity of the moving target. Since for a moving target the radiated signal (the echos reflected of the target) is compressed or stretched out, see figure 2.4, the radar can determine weather the target is moving towards or away from the radar.

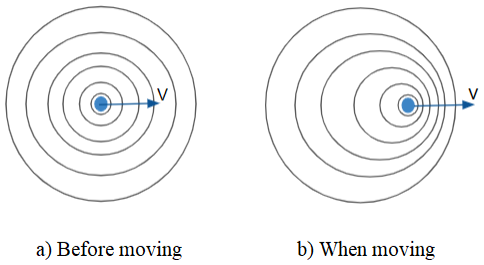

Figure 2.4: Doppler effect of a moving target

Figure 2.4 illustrates that the compressed signals indicate that the target is moving towards the radar, and the stretched out signal indicates that the target is moving away from the radar. Note that the radar can only detect objects with a Doppler velocity relative the radar. Thus objects that fly parallel to the radar will go undetected, due to obstruction by zero-doppler ground clutter.[2].

2.1.1 Electronically Steered Array Antennas (ESA)

ESA radars consists of an antenna array, with several antennas so called antenna elements. There are different types of ESAs, there are passive, active and variant of the active ESA. For a passive ESA all the antenna elements are connected to one single transmiter/receiver, this works due to the individual phase shifters connected to each single antenna element. Phase shifters are modules that generates phase shifts to correct the phase lag of the waves due to the distance between the antenna elements[12]. This master thesis will focus on STAP for clutter suppression which is applicable on active ESA(AESA).

For an AESA the antenna elements are all connected to individually transmitters/receivers, see figure 2.5. Compare to the basic single antenna model with one common transmitter and receiver in figure 2.1. With individually T/R modules one is able to steer the beam(the energy direction) in desirable directions without moving the antenna arrays. This is done by individually controlling the phase shifts digitally of the waves transmitted and received by each antenna element [11].

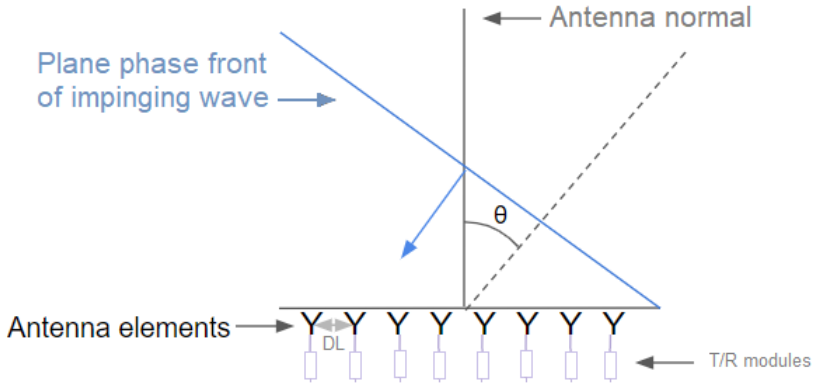

Figure 2.5: AESA

Since an ESA can be mounted on a fixed position on an aircraft structure and still steer the beam there is no need for drive motors or rotary joints. These are all possible sources of failure. By reducing these sensitive parts one has increased the reliability. Since there is no inertia that must be considered when steering the beam one can easily and very fast change the direction of the beam. The ESA beam can be positioned anywhere within its range in less than a millisecond. Compared to other antennas when changing the direction of the beam's motion takes about a tenth of a second [12].

Since each antenna element individually transmits waves interference occurs. Interference is a wave phenomena that occur when two or more waves overlap in the same region and interacts. Signals are amplified or cancelled out[2]. One takes advantage of this interference when controlling the beam[12]. As mentioned earlier the beam is digitally controlled by changing the phase-shifts of the waves. Figure 2.6 illustrates this.

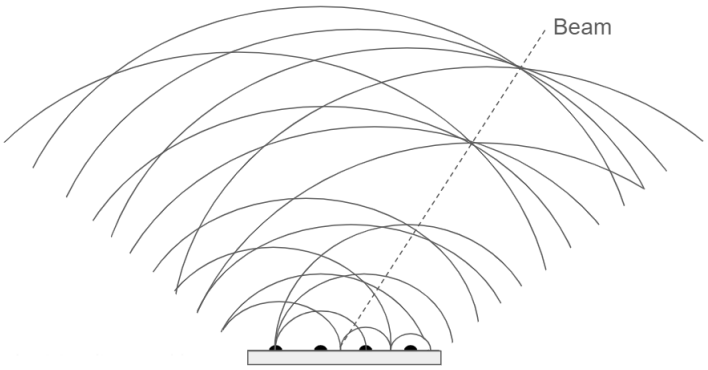

Figure 2.6: Illustration of steering the beam of an ESA

As figure 2.6 illustrates, the transmitted waves travels in different directions. Here the beam is when the signal strength reaches a maximum due to interference, this is called the *mainlobe*. Other lobes are present too due to local maximums, but with less energy called *sidelobes*[12]. Figure 2.7a) illustrates these lobes and their directions for the case when the beam is steered to the broadside of the antenna array.

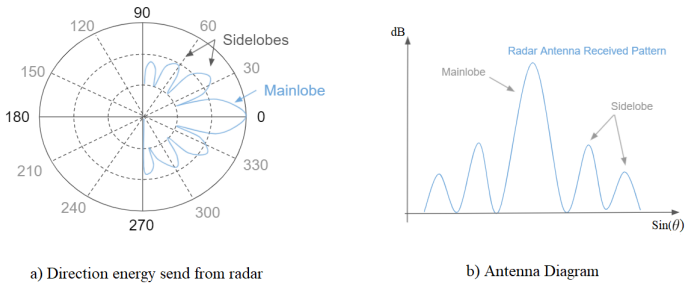

a) Direction energy send from radar

b) Antenna Diagram

Figure 2.7: Illustration of mainlobe and sidelobes

In figure 2.7b) an antenna diagram of the received signal from figure 2.7a) is shown. Here one clearly can identify the main lobe and side lobes. This is not always the case. When the received signal includes clutter some lobes contains more energy, which makes it more difficult to distinguish the target. [12]. For this thesis the assumption is made that the target is found in the mainlobe.

2.2 Signal Processing

Signal processing is essential for a radar system. With signal processing data are transformed to knowledge. The incoming signals will probably consists of the signal reflected from the target, noise from the receivers itself and other unwanted reflected signals. These unwanted reflected signals are as mentioned earlier called clutter. Clutter can come from anything in the surroundings, for example cars or the ground. The ground generates a lot of clutter. [1] Signal processing can be used to filter out unwanted signals. There are several methods for signal processing. This report will look at STAP, using post-doppler processing.

2.2.1 Signals

Let's start with the most general mathematical formula for a cosine signal, which is:

$$X(t) = A\cos(wt - \alpha) \tag{2.2}$$

Here A denotes the amplitude of the wave, $w = 2\pi f$ denotes the angular frequency and α the phase shift. If the signal would move among, for example an y-axis, the formula would become:

$$X(t) = A\cos(ky - wt - \alpha) \tag{2.3}$$

Here $k = \frac{2\pi}{\lambda}$. The negative sign before wt indicate that the wave travels in a positive direction relative the y-axis [2]. For now the direction of the wave is not interesting, but this is good to remember for later in the report. However, in complex analyze one often express the signals using Euler's formula:

$$e^{j\theta} = \cos(\theta) + j\sin(\theta) \tag{2.4}$$

Take the reverse Euler relation for $\cos(\theta)$ and one get:

$$\cos(\theta) = \frac{e^{j\theta} + e^{-j\theta}}{2} \tag{2.5}$$

Applying reverse Euler on equation (2.2) gives[5]:

$$\cos(\theta) = \frac{1}{2}\left(e^{j(wt+\alpha)} + e^{-j(wt+\alpha)}\right) \tag{2.6}$$

Note that equation (2.6) has a symmetric Fourier transform, which is illustrated in figure 2.8. Why Fourier transform of a wave is interesting for radar applications will be explained shortly in chapter 2.2.2.

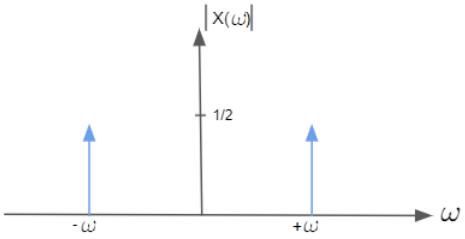

Figure 2.8: Symmetry of Cosine signal

The minimum sampling rate for reconstruction of a signal is a sampling frequency twice the signal frequency, which called the Nyquist rate[5]. For radar application this results in high frequencies. To avoid the high frequencies the signal can be "moved" and centralized by frequency modulation. The frequency modulation is done by multiplying equation (2.2) with e^{jw_0t} [5]:

$$X_m(t) = X(t)e^{jw_0t} = \frac{1}{2}\left(e^{j((w+w_0)t+\alpha)} + e^{-j((w-w_0)t+\alpha)}\right) \tag{2.7}$$

The first part of equation (2.7) will be "moved" to very high frequencies which can be filtered out with a low pass filter, and the second part will be centralized around zero, this is illustrated in figure 2.9.

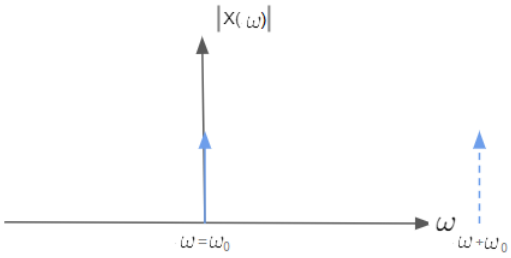

Figure 2.9: Centralizing of the Cosine signal

Nyquist theorem states that a signal can be reconstructed if one samples with at lest the bandwidth, if the center frequency of the original signal is known[13].

Incoming signals of radars

Electromagnetic waves are transmitted and received by the radar antenna. Figure 2.10 illustrates a basic case, with a zero angle, of an incoming signal moving along the y-axis heading towards the antenna elements of an ESA.

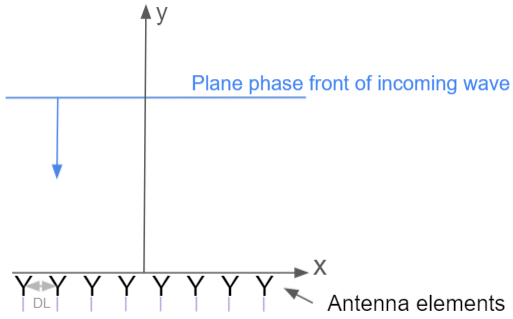

Figure 2.10: Basic incoming signal

The incoming signal in figure 2.10 can be expressed as follows:

$$E(y,t) = E_0 e^{j(k\phi+\omega t)} \tag{2.8}$$

Here E_0 is the power of the electromagnetic field. Note that this basic case results in no phase delay between antenna elements. Since it is a known that the wave is time dependent the equation (2.8) can be simplified:

$$E(y) = E_0 e^{jk\phi} \tag{2.9}$$

Note that for an ESA one does not transmit or receive one single signal. Each antenna element will individually transmit/receive a signal. Thus, when receiving the radar will get a sum of signals. Which can be written as:

$$E(y) = E_0 \sum_{n=1}^{N} e^{jk\phi} \tag{2.10}$$

Here $n = 1, 2, \ldots, N$ is the number of antenna elements. However most received signals have a non-zero angle, see figure 2.5. For a signal with an angle, one uses trigonometric relations to get an expression for y.

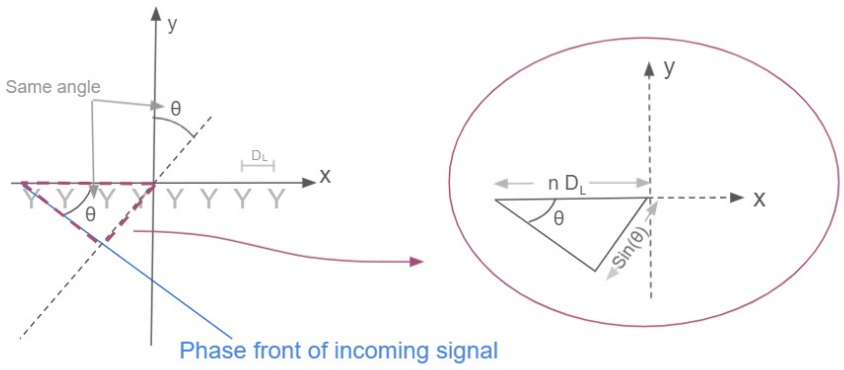

Figure 2.11

Figure 2.11 illustrates the phase front of incoming signal when it reaches the left antenna element. From this figure the phase difference between element positions, ϕ, becomes:

$$\phi = D_L nk \sin(\theta) \tag{2.11}$$

Here D_L is the space between each antenna elements (typically $\lambda/2$) and θ is the angle of the incoming signal. Thus, the sum of the incoming signals become:

$$E_{sum} = E_0 \sum_{n=1}^{N} e^{jknD_L sin(\theta)} \tag{2.12}$$

Mentioned earlier that for an ESA each received signal is individually weighted. Thus, the sum of the incoming signals become:

$$E_{sum} = E_0 \sum_{n=1}^{N} w_n e^{jknD_L sin(\theta)} \tag{2.13}$$

Here w_n is the individually weight for each element.

2.2.2 Signal Processing for Radar systems

Simplified signal processing chains are illustrated in figure 2.12. Each box is introduced later. Traditionally one weights and sums the signals from the antenna element before one continuous the process. For both signal processing chains multi-channel processing is required, which is possible using ESA. In figure 2.12 a) a traditional chain is illustrated, while b) shows an alternative chain using STAP.

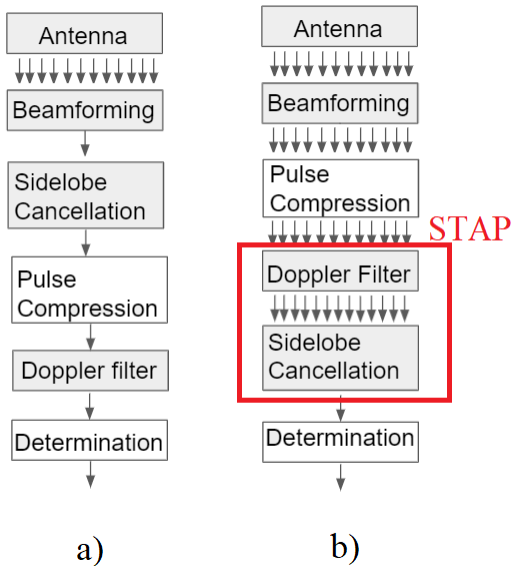

Figure 2.12: Simplifying the signal processing chain

In figure 2.12 a) both space filtering and time filtering is done, but they are done separately. The space filtering and time filtering is done in the *sidelobe cancellation* and *Doppler filter* block respectively. STAP, *Space Time Adaptive Processing*, is a method for space and time filtering at the same time. The math behind STAP will later in this report be introduced.

In figure 2.12 the channels are represented by arrows. Note that model 2 require more computer power for the calculations. To do this one need to update the Sidelobe cancellation block, the other parts of the signal processing chain in figure 2.12 will not be changed for this master thesis. The white blocks in figure 2.12 will not be simulated at all, since they are not a crucial part for analysing STAP.

Beamforming

Beamforming is another word for steering the beam. Which for an ESA is usually done digitally.[10] Figure 2.13 illustrates the digital beamforming. As mentioned earlier the digital beamforming is done by digitally compensate the phase shifts of the transmitted signals to create wave interference as desired, remember figure 2.6.

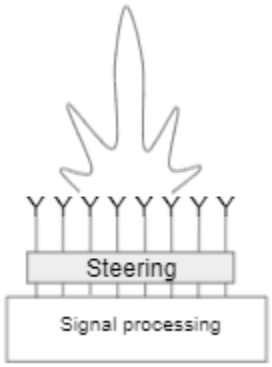

Figure 2.13: Illustration of beamforming of radar.

SLC - sidelobe cancellation

Digital weighing of signals for an ESA is done in the SLC(Beamforming is another name for spatial filtering)[10].

Let's illustrate space filtering in vector form, consider the vectors in figure 2.14 to be the incoming signals in vector form. The blue vector represents the sum of incoming signals described by equation (2.13). The other vector represents the comparing signal, which for the antenna configuration 1 is the signal from a auxiliary antenna(help antenna) and for antenna configuration 2 is the signal tapered in a different way than the original signal.

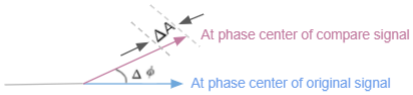

Figure 2.14: Incoming signals in vector form

Here the location of the antenna elements are the phase centers. There is an amplitude difference, ΔA, which is due to gain difference in signals. Also a phase difference, $\Delta\phi$, which is due to difference in distance from clutter to the two phase centers. To counteract the clutter one can start by adjusting the gain of the comparing channel to remove the amplitude difference, see figure 2.15.[12]

Figure 2.15: Adjusted auxiliary gain removes the amplitude difference

Once the amplitude adjustment is done one can move on to the phase adjustment. This is done by adjusting the phase shift in the output of the comparing channel, see figure 2.16. [12]

Figure 2.16: Both amplitude and phase shift are adjusted

One can see that the comparing signal now is 180 degrees out of phase with the clutter signal in the sum channel. Thus, they cancel out. Sometimes one say that a notch has been produced in the antenna's sidelobe pattern in the clutter's direction.[12]

PC - Pulse Compression

Pulse compression is an important part of radar systems. Since radars often send pulses and would like to cover a large area, the pulses would need a very high power. But the system itself has its limitations, due to power supply and transistors etc. Thus one needs another way to represent the pulses, since lowering the power is not an option. This is done by pulse compression [12].

There are several methods for pulse compressing, one commonly used methods is linear frequency modulation. Where the frequency of each transmitted pulse is increased at a constant rate. The received signals has the same linear increase in frequency. The incoming signals passes through a filter that introduces a time lag that decreases linearly with frequency at the exact same rate as the frequency of the echos increases, see figure 2.17 [12].

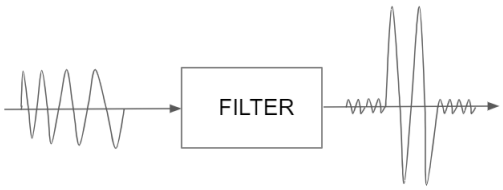

Figure 2.17: Pulse Compression

Again, pulse compression will not be modelled in this thesis.

DF - Doppler filter

Let's take another look at figure 2.2, one cuts out the first transmitted signals and creates a matrix with the intervals between the transmitted signals. This is illustrated in figure 2.18. One dimension represents the number of pulses, and the other dimension represents the time[1]. Both figures illustrated the same thing but in two different ways.

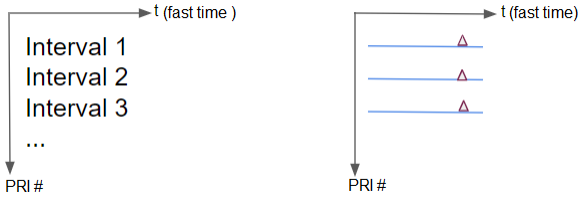

Figure 2.18: Matrix of pulse interval's

The triangles in figure 2.18 illustrates phase shifts from the signals reflected of targets. In practise these signals will not be as smooth as shown above. There will be noise and clutter which makes it harder to detect the phase shifts. However, a continues change in phase shift will result in a frequency. Thus, one way to find the targets phase shifts is to transform the matrix from time domain into frequency domain. This can be done with fast *Fourier transformation(FFT)*. By transforming the matrix into frequency domain one gets the Doppler frequency of the received signals. Most clutter have a Doppler frequency close to zero, for example clutter from the ground. But for the phase shifts from the signals reflected from targets such as other aircraft's will have a significantly larger Doppler frequency, and are much easier to detect in frequency domain[1], see figure 2.19.

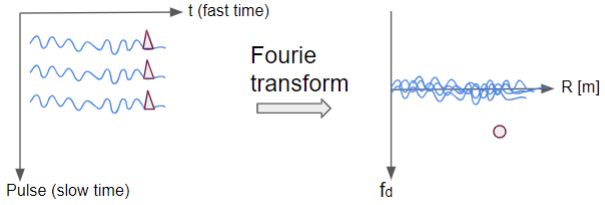

Figure 2.19: Fourier transformation of coherent processing interval(CPI) matrix

One problem is that one will not only get signals reflected of targets, but also reflection from the surroundings. One large source for clutter is the ground. Mentioned before is that the ground mostly has a Doppler frequency close to zero, but some part of the ground will have a similar Doppler frequency to the targets Doppler frequency. [1]

Detection

There are several techniques for detection of a target. A common process is Constant False Alarm Rate (CFAR) detection. CFAR refers to a detection process that estimate interference power by

cells placed nearby a cell to calculate a threshold used to determine if a target is detected in the cell under test[9].

Detection will not be modelled in this thesis.

2.3 STAP - Space Time Adaptive Processing

STAP is an angle-doppler domain filtering technique that is applicable on AESA for clutter suppression. As mentioned earlier a sequence of coherent pulses are transmitted and later received via the antenna array of the radar. The echos received are amplified, down mixed and digitized. This is all done in the individually T/R modules. Then all the signals are individually weighted before forming different antenna channels[6], see figure 2.20.

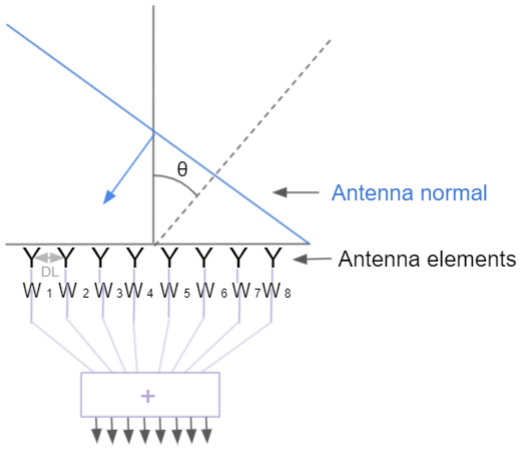

Figure 2.20: Individually weighting the incoming signals for optimal clutter suppression

By applying STAP one adds another dimension to the signal processing. This is illustrated in figure 2.21. To the left is traditionally time filtering illustrated, to the right STAP filtering is illustrated. Compare to figure 2.12, where the traditionally chain sums the incoming signals before processing them with Doppler filtering while the alternative chain processes them separately adding them later using STAP.

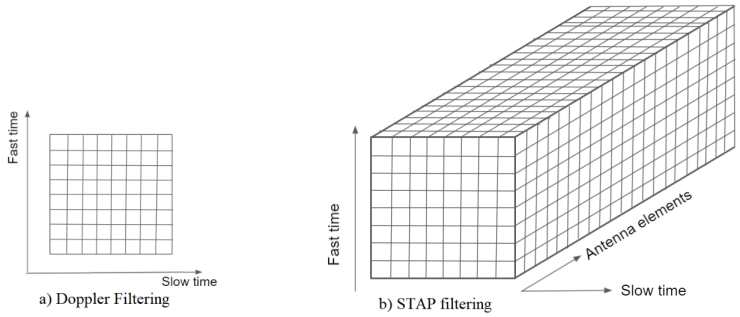

Figure 2.21: STAP filtering using Doppler

By applying STAP one can adapt the clutter filter to the actual clutter received. This is done by estimating the space-time covariance matrix from training data. This matrix contains the covariance between noise and clutter. The clutter is then filtered out and what's left is the signal + noise which is then matched with a Space-Time filter. A test function is designed to be compared to a detection threshold.[6] For this these the target is assumed to be located in the mainlobe, thus the test function is in the direction of the mainlobe.

Let's start by expressing the space-time filter as a two dimensional filter, based on the incoming signal angle(space) and doppler velocity(time). In figure 2.22 a) an airplane with a velocity is illustrated to receive clutter, for an airborne radar looking to the side. The blue dots represent clutter angles. Depending on the angle of the incoming clutter, the clutter will be placed differently in the STAP filter in figure 2.22 b). In figure b) the vertical axis is Doppler velocity and the horizontal axis is the angle of the incoming signal. Note the trend in b) of a straight line. This line represents all possible clutter angles. Since for this thesis the clutter are ground echos and the ground is not on only three marks, but all over.

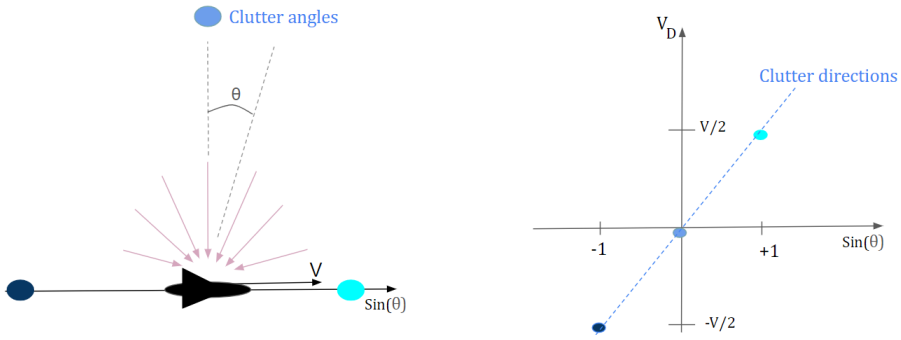

Figure 2.22: Illustration of the relation between the clutter angles and Doppler velocities used in STAP filtering

Now that the relation between the space and time filtering in STAP is introduced let's add a target to the filter, shown in figure 2.23 for an airborne radar looking to the side. For a three dimensional illustration the third axis would be amplitude of the incoming signals.

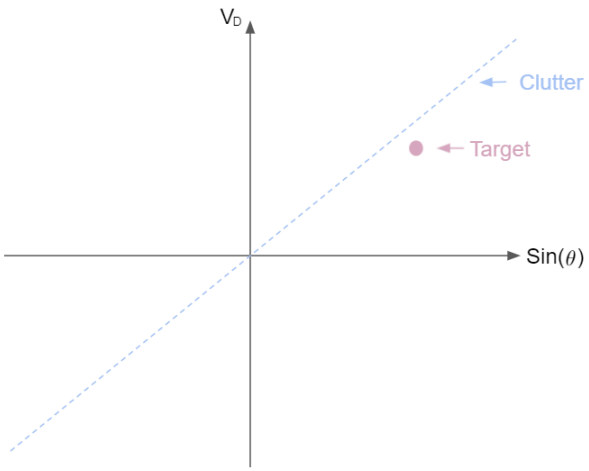

Figure 2.23: Relation between doppler velocity and incoming angle

Using *full STAP* one would calculate one covariance matrix **Q** for the all the angles and Doppler velocities, and it put a series of zeros along the clutter signal. This results in a very large matrix. To avoid the large matrix the *factorized post-Doppler STAP* instead takes a section of the Doppler velocity axis, as shown in figure 2.24. This let's the factorized post-Doppler STAP to calculate with smaller matrices.

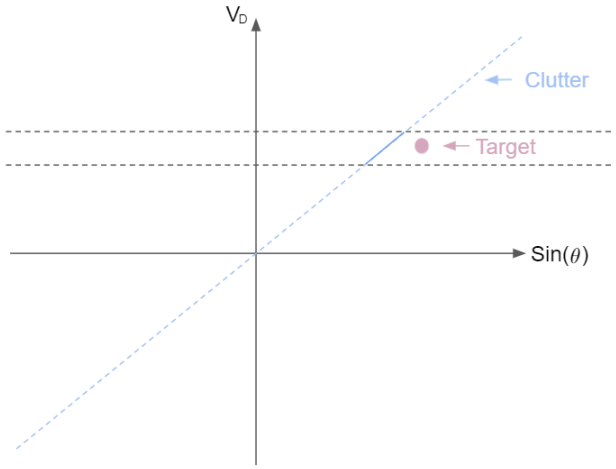

Figure 2.24: Relation between doppler velocity and incoming angle

By using factorized post-Doppler STAP one only needs to cancel out the clutter within the internals while maximising the targets. Doing this through the whole Doppler axis results in an adaptive two dimensional filter equal to a three dimensional filter without the large matrices, see figure 2.25.

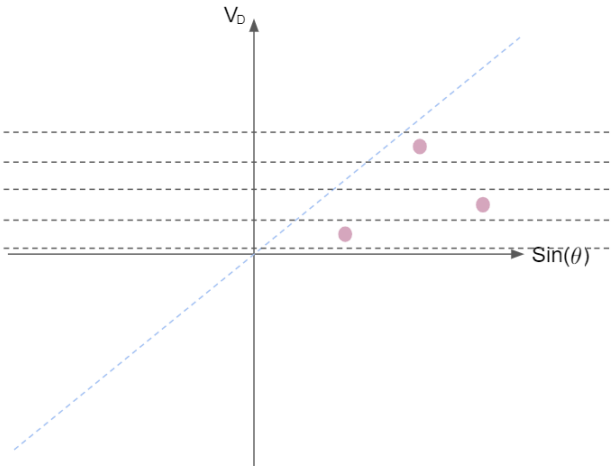

Figure 2.25: Relation between doppler velocity and incoming angle

Thus, Factorized post-Doppler STAP results in less computer power than full STAP.

2.4 STAP algorithm

The following STAP algorithm can be found in *Principles of space-time adaptive processing*, by Richard Klemm published in 2002.

Let's start with introducing the data vector $\mathbf{x}$, which is the input data from the antenna channels after Doppler filtering. This vector consists of a signal vector, $\mathbf{s}$, plus an interference vector, $\mathbf{q}$.

$$\mathbf{x} = \mathbf{q} + \mathbf{s} \tag{2.14}$$

The signal vector $\mathbf{s}$ is the echo from the target, thus it is the signal of interest.

$$\mathbf{s} = \begin{pmatrix} s_1 \\ s_2 \\ \vdots \\ s_N \end{pmatrix} \tag{2.15}$$

Let the interference vector $\mathbf{q}$, it be a mean random vector with a multivariate complex Gaussian distribution.

$$\mathbf{q} = \begin{pmatrix} q_1 \\ q_2 \\ \vdots \\ q_N \end{pmatrix} \tag{2.16}$$

The interference vector has a correlated part, $\mathbf{c}$, which can be jammer or clutter. And an uncorrelated part, $\mathbf{n}$, for example receiver noise. Both parts assumed to be multivariate complex Gaussian distribution. The vector $\mathbf{q}$ becomes:

$$\mathbf{q} = \mathbf{c} + \mathbf{n} \tag{2.17}$$

Thus the vector $\mathbf{x}$ becomes:

$$\mathbf{x} = \mathbf{c} + \mathbf{n} + \mathbf{s} \tag{2.18}$$

The interesting part of $\mathbf{x}$ is the signal vector $\mathbf{s}$, but the signal vector $\mathbf{s}$ is unknown. How does one find what one is looking for, if one does not know what it looks like? This is done by coming up with a hypotheses of what the signal vector might look like. This is done by creating a *search beam*, $\mathbf{S}_b$, this vector is chosen based on the antenna configuration. The search beam is modeled target response without clutter and nosise, by applying a well-known linear weighting on $\mathbf{x}$.[6](Derivation of this linear weighting can be found in appendix A):

$$\mathbf{W}_{opt} = \mathbf{Q}^{-1}\mathbf{S}_b \tag{2.19}$$

Where $\mathbf{Q}$ is the interference covariance matrix:

$$\mathbf{Q} = \begin{pmatrix} q_{11} & q_{12} & \cdots & q_{1N} \\ q_{21} & q_{22} & \cdots & q_{2N} \\ \vdots & \vdots & \ddots & \vdots \\ q_{N1} & q_{N2} & \cdots & q_{NN} \end{pmatrix} \tag{2.20}$$

The coveriance matrix, $\mathbf{Q}$, is a matrix giving the covariance between each pair of elements. For STAP the covariance matrix describes the estimated relations between clutter and noise in the channels. $\mathbf{Q}$ is estimated by weighting the matrix product of $\mathbf{q}$ multiplied with its hermitian conjugate, and divided by the the number of samples, M [7]:

$$\mathbf{Q} = \frac{1}{M}\mathbf{q}\mathbf{q}^H \tag{2.21}$$

The optimal weighted signal becomes:

$$y = x^* Wopt \tag{2.22}$$

One way of suppressing of clutter is using the *subspace technique*. Which is one way to scale down the vector space to an acceptable subspace and then perform interference rejection at the subspace level. This can be done with a corresponding linear transform $\mathbf{T}$. [6] Note that this $\mathbf{T}$ will differ for the two antenna configurations. However, for both configurations the transform matrix is applied on the following vectors.

$$\mathbf{s}_T = \mathbf{T}\mathbf{s} \tag{2.23}$$

$$\mathbf{q}_T = \mathbf{T}\mathbf{q} \tag{2.24}$$

Note that no energy must be lost during the optimal interference suppression performance. Here the search beam is used again. The transformation matrix should therefore contain a beamformer weighting that are matched to the expected signal, again the search beam $\mathbf{S}_b$ is used. This means that the $\mathbf{T}$ depends on the signal direction. Adaption of the $\mathbf{Q}_T^{-1}$ has to be conducted separately for all individual directions.

The optimum weighting becomes:

$$\mathbf{W}_{optT} = \mathbf{Q}_T^{-1}\mathbf{S}_{bT} \tag{2.25}$$

Note that so far the model uses an estimated covariance matrix $\mathbf{Q}$ based on the training data. The training data is data collected by the radar. The radar transmits and receives several signals, analysing and uses them as training data to get an understanding of the conditions of the surroundings. Once the radar has an understanding of the surroundings it can provide correct information about moving targets. The radar is desirable to be as quick as possible. Thus, as few training data as possible is desirable. The estimated $\mathbf{Q}$ depends on the size of training data set. This thesis will analyze the performance of the STAP model when decreasing the size of the training data set. This

can be done by comparing the estimated $\mathbf{Q}$ with the true $\mathbf{Q}_{true}$. One way do to this is calculating the improvement factor for the weighting of the signals:

$$IF = \frac{SNR_{out}}{SNR_{in}} = \frac{\mathbf{w}_T^H \mathbf{S}_{bT} \mathbf{S}_{bT}^H \mathbf{w}_T tr(\mathbf{Q}_{true})}{\mathbf{w}_T^H \mathbf{Q}_{true_T} \mathbf{w}_T \mathbf{S}_b^H \mathbf{S}_b} \tag{2.26}$$

The optimal improvement factor[6]:

$$IF_{opt} = S_b^H \mathbf{Q}_{true}^{-1} S_b \frac{tr(\mathbf{Q}_{true})}{S_b^H S_b} \tag{2.27}$$

The fraction of these improvement factors IF/IF_{opt} will show how close the estimated covariance matrix is to the true covariance matrix.

$$IF_{norm} = \frac{IF}{IF_{opt}} \tag{2.28}$$

By decreasing the size of the training data set one can analyse when the model will stop generate an acceptable estimated $\mathbf{Q}$. The size of the training data set will later be compared to the size of the training data set of the other model analysed in this report. As mentioned earlier, the main purpose of this master thesis is to compare these two models and analyse which of these will be able to generate the best estimated $\mathbf{Q}$ with the smallest training data set.

When simulating STAP applied on the antenna configurations models in Matlab, the input vector becomes:

$$x = E_0 \sum_{n=1}^{N} b_n^k e^{j\left(\frac{2\pi}{\lambda} n D_L \sin(\theta) - \omega t\right)} \tag{2.29}$$

Which looks familiar, remember equation (2.13). The difference here is the multi-channel processing. Here k is the channels and b is the beam forming weights from the respective transformation matrices.

2.4.1 Tapering

Tapering is an important part of signal processing for radar systems. Tapering reduces the side lobes that occur for leakage from the main lobe. There are several taperings in use, but the Taylor tapering is often used in radar applications. [3] The trade off between side lobe level and main lobe level is desired to adapt the radar unit to work optimally for each application.

There are many ways to do this. There are also a new ideas of how one could improve today's concepts for the future. This master thesis report will compare two antenna configurations using different kind of taperings. As mentioned earlier the purpose of this master thesis is to compare two configurations using STAP for clutter suppression for airborne radar systems. The comparison will be done on the sizes of training data needed for the methods to still be able to generate an acceptable estimated coveriance matrix.

Chapter 3

Method

For analysing the two configurations a Matlab models was used. Since the purpose of this thesis was to analyse the two configurations using STAP only basic antenna configurations were made. There were no complete radar models made. However, the matlab models both would:

- Varying amount of training data
- Calculate the coveriance matrix **Q**
- Calculate the weights
- Apply the weights

The comparison of the two antenna configurations was done on the sizes of training data needed for the configurations to still be able to generate an acceptable estimated coveriance matrix and calculating Signal to interference and Noise ratio.

3.1 Antenna Configuration 1 - Auxiliaries

As mentioned before, the first Antenna Configuration is based on auxiliary channels. In figure 3.1 a) is a single sum channel pattern illustrated, as one can see it will be a sinc curve. One axis is the antenna gain in decibel (dB), the other axis is the direction of the incoming signal in the form of $sin(\theta)$.

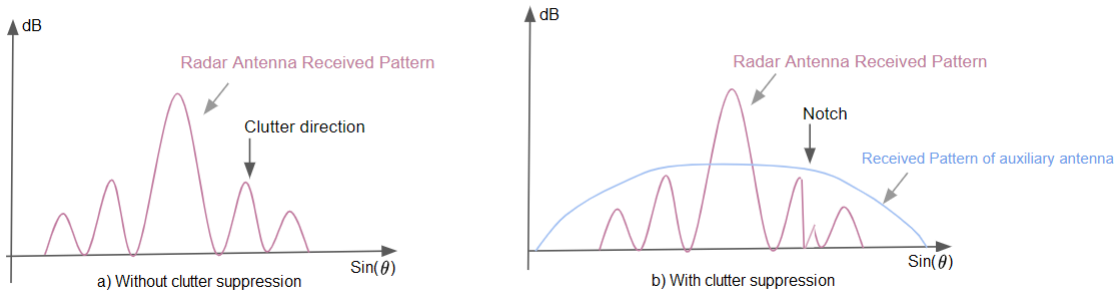

Figure 3.1: Clutter suppression in the antenna received pattern

In b) of figure 3.1 one can also see the received pattern of an auxiliary channel. An auxiliary channel contains data from auxiliary antenna. The gains for the auxiliary antenna and the main antenna of the radar can be compared in the clutter directions. This is done by estimating the covariance matrix containing the statics of the clutter signals. By doing this one gets an understanding of how much of the sum-signal from main antenna is clutter, and one can do something to counteract the clutter signals [12]. Remember the sidelobe cancellation described in chapter 2.2.2, where the clutter signals has been cancelled out one says a notch has been placed as shown in figure 3.1. For an ESA radar one can choose one or several antenna elements to be used as auxiliary channels, which is done in this report.

Transformation Matrix $\mathbf{T}_1$

Earlier is the linear transformation matrix $\mathbf{T}$ mentioned. This matrix is applied in equations (2.23) and (2.24). The suitable transformation matrix for the auxiliary configuration is the following matrix [6]:

$$\mathbf{T}1 = \begin{pmatrix} b_{11} & 1 & \dots & 0 \\ b_{21} & 0 & \dots & 1 \\ \vdots & \vdots & \ddots & \vdots \\ b_{N1} & \dots & 1 & 0 \end{pmatrix} \tag{3.1}$$

Where the first column is the weighting coefficients, also called the beamforming coefficients of the sum beam. These weight can be only phase or include some amplitude tapering, in this thesis it will be taylor tapered which is often used in radar applications like weighting and antenna design.[3] The other columns represents the antenna elements to be used as a auxiliary channels.

As mentioned in chapter 2.4 the search beam vector is chosen based on the antenna configuraiton. Both search beam will be places in the mainlobe, since for this thesis the assumption is made that the target is in the mainlobe. For the auxiliary configuration the search beam is chosen as follow:

$$S_{bAUX} = \begin{pmatrix} E_{sum}(\theta = 0) \\ 0 \\ \vdots \\ 0 \end{pmatrix} \tag{3.2}$$

3.2 Antenna Configuration 2 - DPSS

The second Antenna configuration is based on multitapering using discrete prolate spheroidal sequences(DPSS). Which varies the tapering on the incoming signal using a tapering set. Instead of comparing the sum channel to auxiliary channels, one apply different tapers on the sum signal and compare the tapers. Figure 3.2 illustrates the Matlab function *dpss* when four taperings are applied. Each tapered signal in the figure is one channel, thus for four taperings will be four channels.

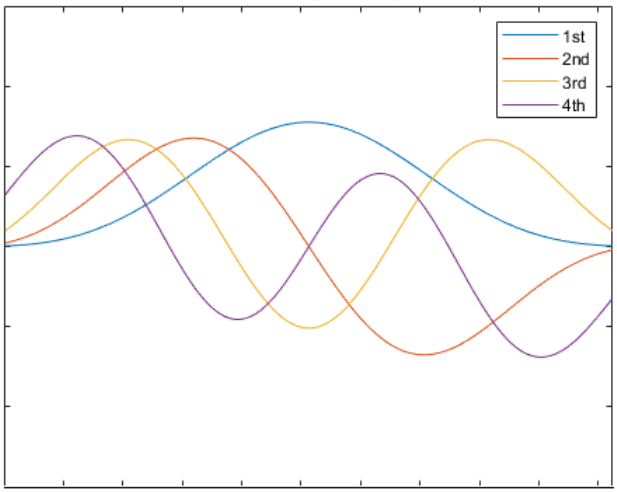

Figure 3.2: DPSS illustrated when four tapers are used, figure from *mathworks.com*

The discrete prolate spheroidal or so called slepian sequencies is derived from the following time-frequency concentration problem:

$$\lambda = \frac{\int_{-W}^{W} |X(f)|^2 df}{\int_{-Fs/2}^{Fs/2} |X(f)|^2 df} \tag{3.3}$$

Where Fs is the sample rate and $|W| < Fs/2$. This ratio determines which index-limited sequence has the largest proportion of its energy in the band $[-W, W]$. For index-limited sequences, the ratio

must satisfy the inequality $0 < \lambda < 1$. The first discrete prolate spheroidal sequence maximizes this ratio. The rest of the sequences maximizes the ratio and are orthogonal to all other sequences. Thus, one forms an orthogonal set of bandlimited sequences[4].

Transformation Matrix $\mathbf{T}_2$

The suitable transformation matrix for the multitapering configuration is:

$$\mathbf{T}2 = \begin{pmatrix} b_1^1 & b_1^2 & \dots & b_1^N \\ b_2^1 & b_2^2 & \dots & b_2^N \\ \vdots & \vdots & \ddots & \vdots \\ b_N^1 & b_N^2 & \dots & b_N^N \end{pmatrix} \tag{3.4}$$

Where each column is weighted with different discrete prolate spheroidal sequences. The columns in **T2** are used as the channels for STAP application. This matrix is applied on the same equations as transformation matrix $\mathbf{T}1$, thus equations (2.23) and (2.24).

The search beam for the DPSS simulations is chosen to be the values of the taperings in the direction of the mainlobe, which for this thesis is located at $\sin(\theta) = 0$.

$$S_{bDPSS} = \begin{pmatrix} E_1(\theta = 0) \\ E_2(\theta = 0) \\ E_3(\theta = 0) \\ E_4(\theta = 0) \end{pmatrix} \tag{3.5}$$

Chapter 4

Result

As mentioned in Chapter 3, a matlab model was used. Again, only the sidelobe cancellation part of radar signal processing was modelled for both configurations. In general for simulations four channels were used. Thus for equation (2.29) k=4, resulting in a matrix with four columns. Each column represent a channel. For simulations the configurations suppresses the maximum number of four clutter signals.

For both configuration the AESA was designed with following properties:

- 20 antenna elements, which were linearly spaced (half a wavelength apart)
- The "true" covariance matrix calculated using 1000 samples
- The estimated covariance matrix calculated using 0-100 samples
- Mean values of 10 simulations were used for all calculations of clutter rejection performance

Assumptions :

- Only one target in sight
- The target is located in the mainlobe
- No other interference than the added clutter
- Noise signal is white Gaussian noise
- Clutter signal is Gaussian noise

4.1 Auxiliary Configuration

As mentioned four channels where used in the following simulations, where three of them where auxiliary channels. Starting with analysing the basic case for the antenna configuration, which is a single clutter signal. Figure 4.1 illustrates the original antenna diagram, the adaptive antenna diagram, the three auxiliary antenna diagram and the clutter direction for this simulation. Clearly the configuration has zeroed the adapted signal at the direction of the clutter. Note that the sidelobes are increased for the adapted signal, due to the suppression of clutter. For this thesis this is not a problem. Since no other interference directions exists here.

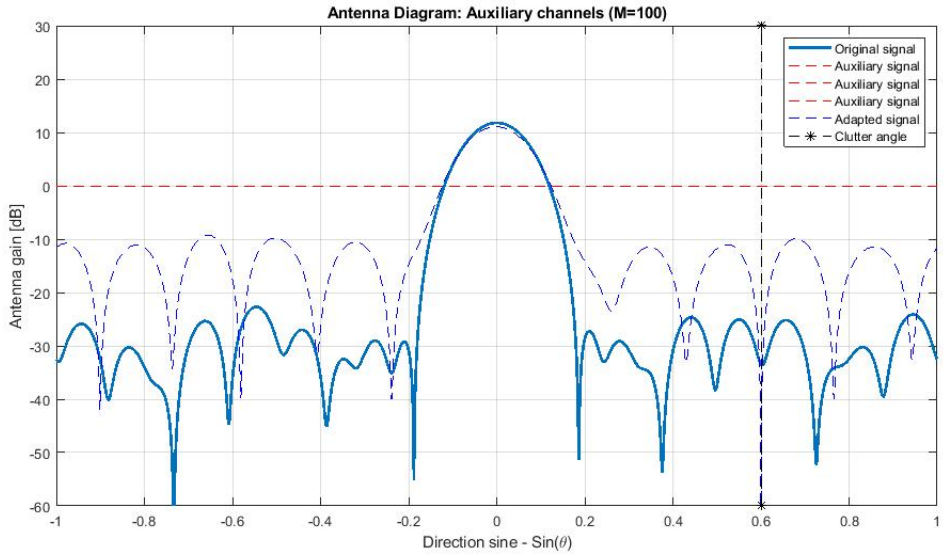

Figure 4.1: Antenna diagram of Configuration 1 - Auxiliary configuration. *Blue curve - original, blue doted curve - adapted, red doted line - auxiliary(all three are very close, thus only one line is visible), black doted line - clutter angle*

The auxiliary channels in figure 4.1 results in a constant gain of 0 dB. Since the auxiliary channels only uses one single antenna element their antenna diagram will result in a very wide pattern. This pattern appears in the figure to be a straight line. As mentioned earlier, the *normalised improvement factor(IF)* is one way to analyze the effectiveness of the weighting of the signals. Figure 4.2 shows the IF and also the *signal to interference and noise ratio(SINR)* for the first antenna configuration using STAP for a variant number of samples used in the training of **Q**. Here the SINR reaches a stable level at about 12-13 dB.

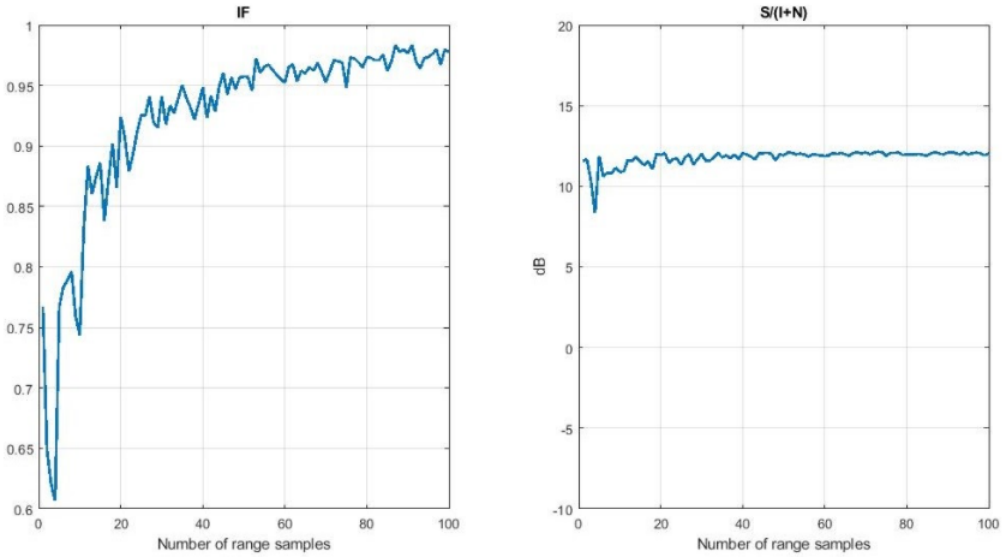

Figure 4.2: To the left is the *IF* shown and to the right the *SINR* for Auxiliary configuration simulation. Both plots illustrates how the auxiliary configuration behavior improves when increasing the number of range samples

The IF curve stabilizes at around 40 number of samples. Remember that four channels were used in these simulations. Thus, it seems that at least ten times the number of channels is required as samples for this configuration to generate an estimated covariance matrix that gives 95% of the full performance. Further simulations were made to confirm this theory. The only thing changed for these simulations were the number of channels used, see figure 4.3. Here the improvement factor is plotted for a variant numbers of channels. Clearly the more channels used in simulations the more samples were required for the estimation of the covariance matrix.

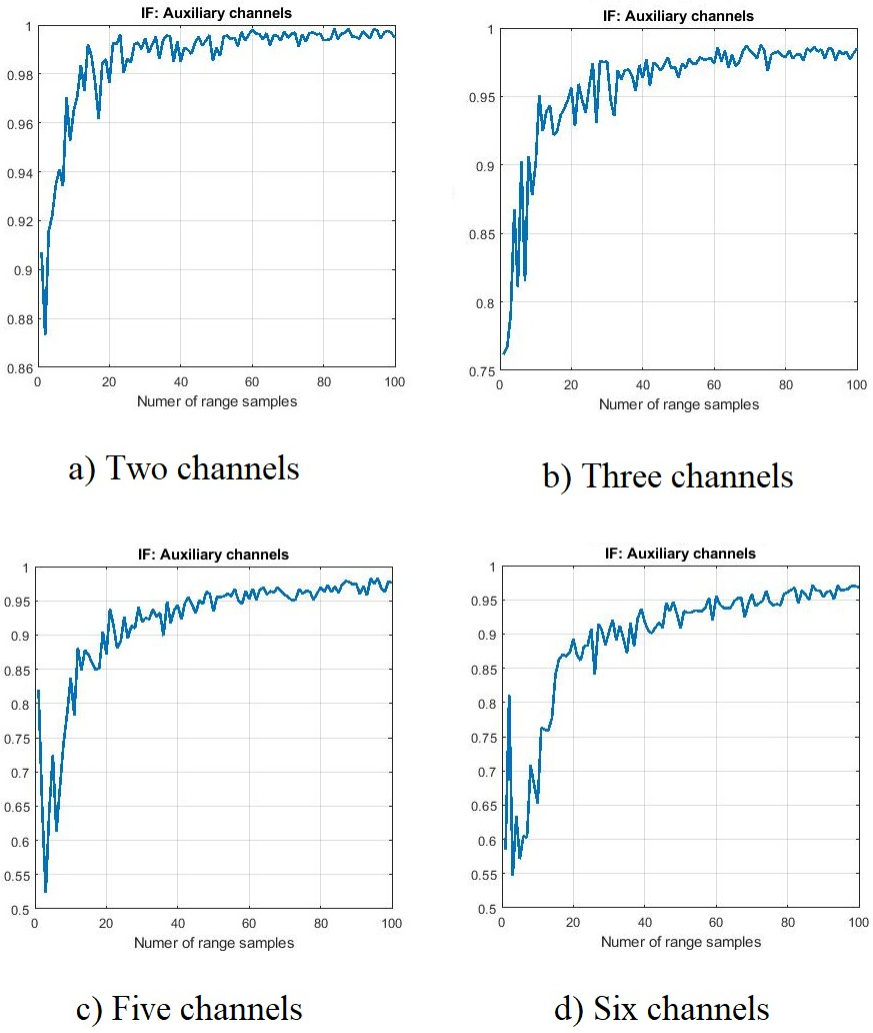

Figure 4.3: Varying the number of channels in simulations for auxiliary configuration in basic case with one single clutter angle

4.2 DPSS Configuration

As mentioned earlier there were four channels for these simulations. For the DPSS configuration this means the incoming signals were weighted with four different DPSS. In figure 4.4 one can see that the clutter adapted signal has zeroed out the signal in the clutter direction.

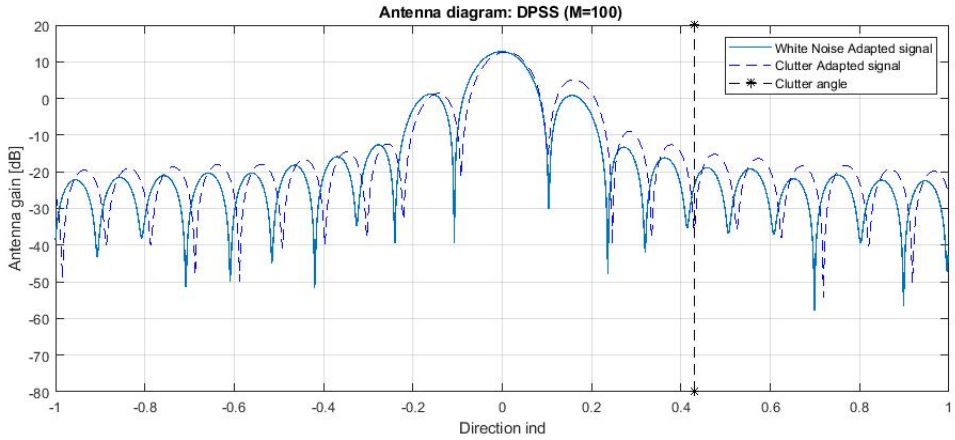

Figure 4.4: Antenna Diagram of Antenna configuration 2 - DPSS , *blue curve - original, blue doted curve - adapted, black doted line - clutter angle*

Note that in figure 4.4 the clutter adapted signal is compared to a white noise adapted signal. The improvement factor and signal to interference and noise ratio for the simulation above is plotted in figure 4.5. Again, IF stabilizes around 40 samples. When varying the number of channels for the DPSS configuration one get a similar behavior of the IF as for the Auxiliary configuration. Thus, the more channels used in simulation the more samples were required for the configuration to stabilize IF. Figure 4.5 also shows the SINR for figure 4.4, that stabilized around 12.5 dB.

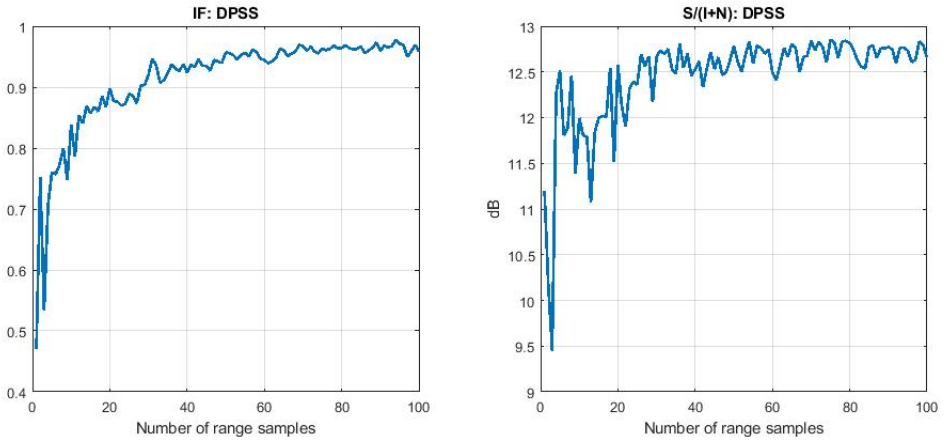

Figure 4.5: To the left is the *IF* shown and to the right the *SINR* for DPSS configuration simulation. Both plots illustrates how the DPSS configuration behavior improves when increasing the number of range samples

Simulations showed occasionally displacements of the notch. Multiple simulations indicated that a small displacements of the notch to be a repeatedly occurrence for the DPSS configuration. However, when displacement occurred the notch was often still close enough to the clutter direction to generate a noticeable power difference between the white noise adapted and Gaussian adapted signal, see figure 4.6.

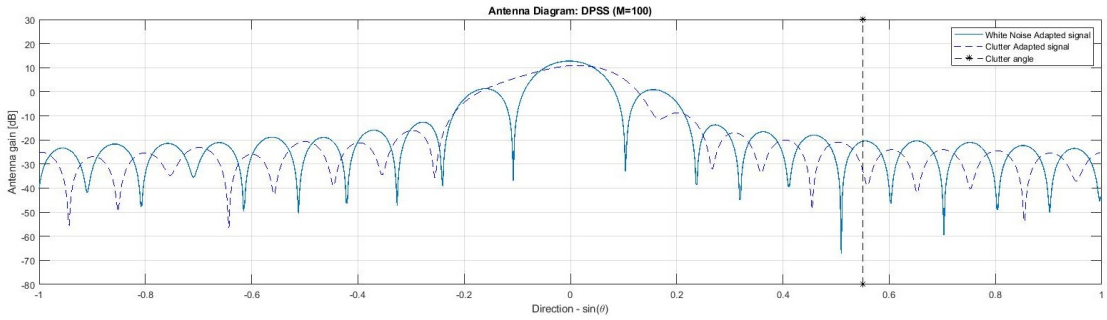

Figure 4.6: DPSS configuration generated a small displacement of the zero in the clutter direction for the adapted signal

The bigger problem with the DPSS configuration showed to be the occasionally complete fail of canceling out the clutter signal completely, this is illustrated in figure 4.7.

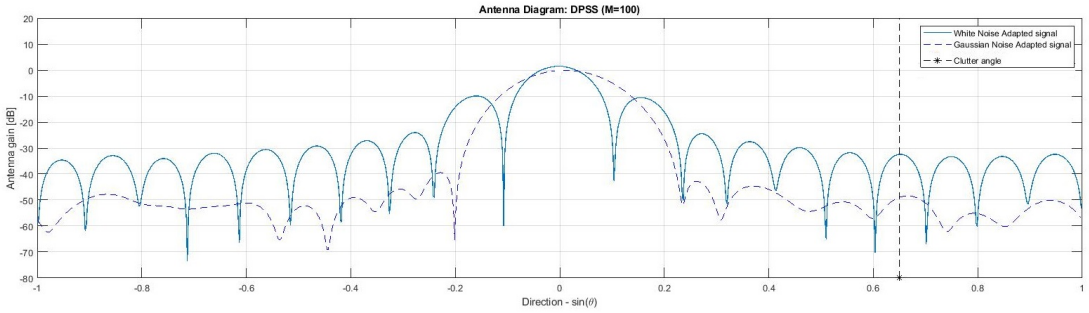

Figure 4.7: DPSS fails to place a zero at the direction of the clutter for the adapted signal

As mentioned in chapter 2.2.2 one uses the Fourier transform of the incoming data to identify the clutter signal when time filtering. For configuration 2 this means that all four channels that are tapered with different DPSS are Fourier transformed. Analysing the Fourier transform of these taperings for the failed DPSS simulation showed that two taperings had a zero close to the clutter angle, this means that two channels has no information about the clutter. The same channels had zeros in the mainlobe, which means that the two channels had no information about the target. Thus, two taperings contributes with no information about the target or clutter signal. With only two taperings left the DPSS need to compromise. Again, the DPSS seldom failed to suppress clutter.

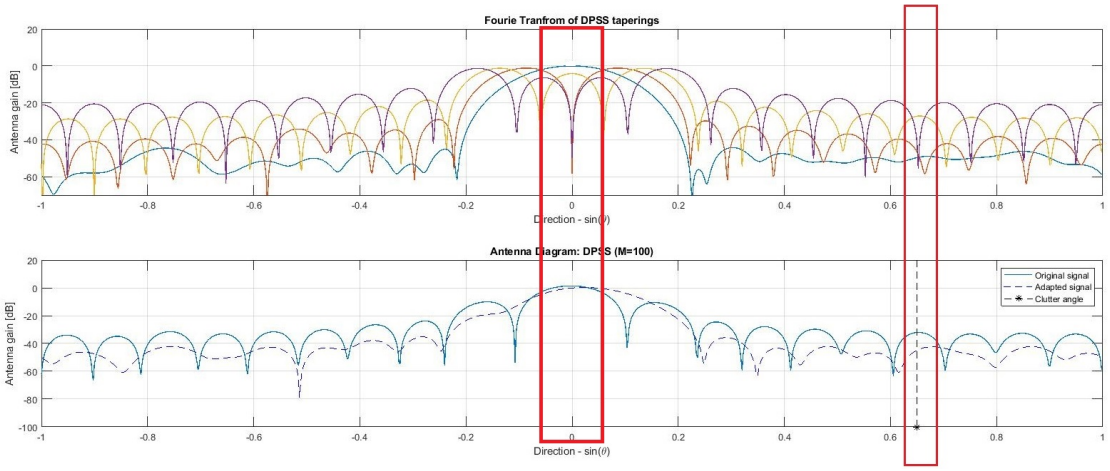

Figure 4.8: Fourier transforms of the taperings in the channels shown in the top plot for a DPSS fail. In the bottom plot is the fail to zero out the clutter shown

More simulations indicated also that the DPSS configuration could occasionally zero out the clutter even though two tapering generated no information regarding the target or clutter. Again, compromise had to be made. Figure 4.9 shows the DPSS suppression of the clutter resulted in a lost

of 3 dB in the mainlobe.

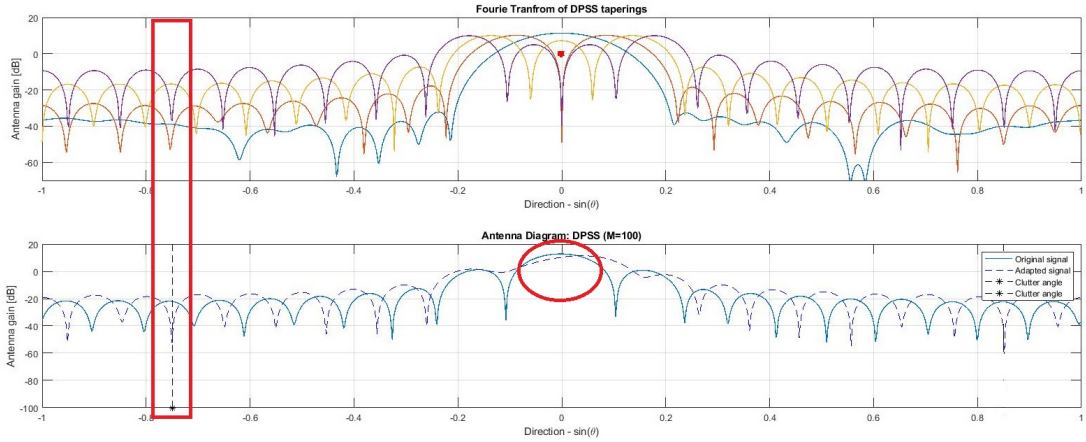

Figure 4.9: DPSS compromising for when taperings have no information

4.3 Comparison between the two configurations

The same conditions were applied for both configurations for comparison simulations. Same clutter signal power, same number of clutter signals, same clutter signals directions and same number of channels.

4.3.1 Single clutter signal

There are two cases of a single clutter signal that are of interest. First, when the clutter direction is far from the mainlobe. Second, when the clutter direction is close to the mainlobe. Which can be a challenge for the configurations. Since they need to put a notch where there is clutter while maximizing the power of the mainlobe.

Clutter angle far from mainlobe

Figure 4.10 illustrates how the two configurations performs when the single clutter direction is far form the mainlobe. The direction of the clutter signal for these simulation is $sin(\theta) = 0.78$ (44.7 deg). Both configurations handles this case well. They both reduce the clutter signal while keeping the mainlobe power.

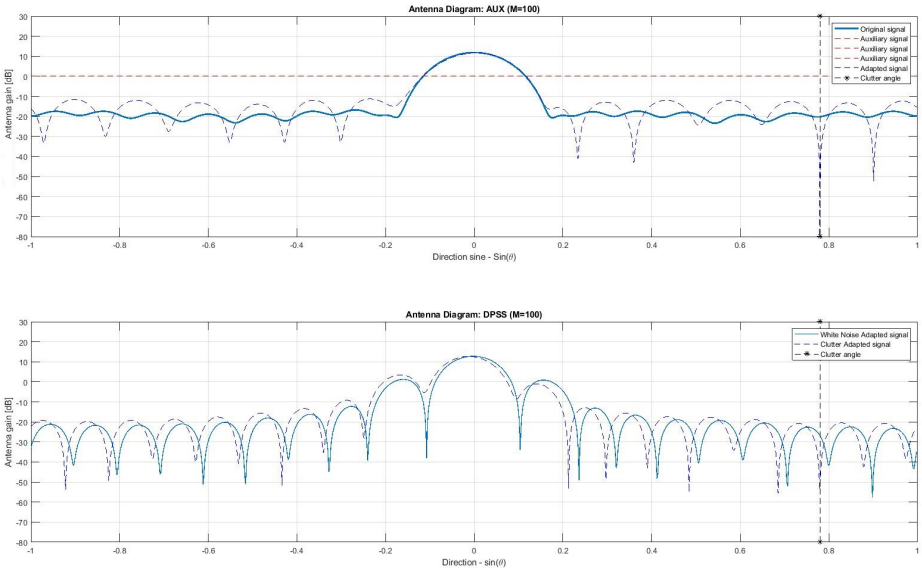

Figure 4.10: Single clutter angle far from mainlobe comparison. The top plot shows the auxiliary configuration, the bottom plot is the DPSS configuration.

Improvement factor and signal to interference and noise ratio for both configuration for this single clutter signal far from mainlobe, is shown in figure 4.11. The two configurations shows a similar IF

behavior for the two configurations. Based on figure 4.11 one could clearly conclude that the DPSS generated a higher SINR than the auxiliary configuration. However, the DPSS generates a more unstable SINR for the first 20 number of range samples. Monte Carlo simulations also indicate that the DPSS varies more between simulations than the auxiliary configuration. Thus, the auxiliary generates more stable results. The Monte Carlo simulations shows the standard deviation of the SINR for both configurations.

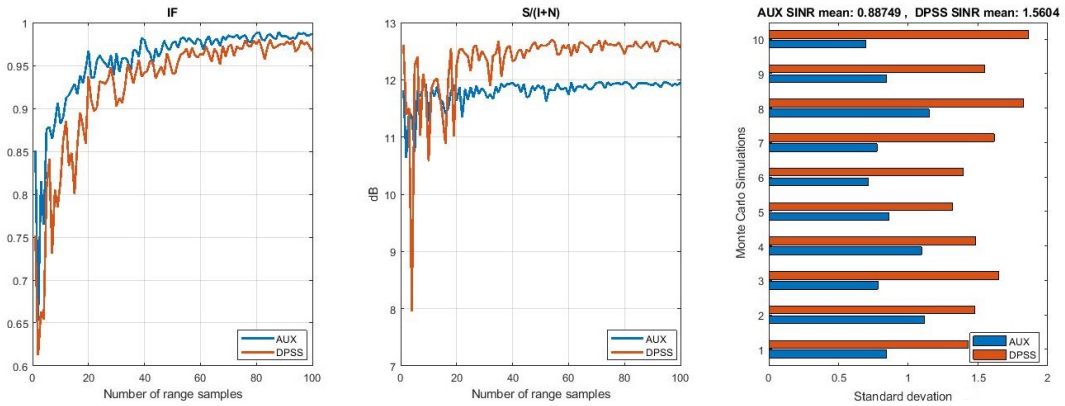

Figure 4.11: IF, SINR and standard deviation of SINR for simulation shown in figure 4.10, comparison of the two configuration in the case of one single clutter angle far from mainlobe

One could wonder about which configuration generates the larger decibel change for the notch. In the table below are the difference in dB listed for multiple simulation with the exact same conditions. For every simulation the auxiliary configuration generated the "deeper" zero. Thus, one conclusion is that the auxiliary configuration generates more distinct notches.

AUX	-53.09	-30.77	-30.38	-27.72	-57.04	-45.22	-37.76	-50.78	-25.19	-38.76
DPSS	-9.64	-27.67	-21.77	-17.09	-35.85	-23.17	-30.39	-20.48	-11.07	-15.90

Simulations also indicate that the auxiliary configuration performed better for clutter signals with low power. The DPSS configuration struggled with clutter signals of 13dB or less. For which the DPSS seldom succeeded cancelling out the clutter signal.

Clutter in the mainlobe

Analysing how the two configuration performance changes when the single clutter signal approaches the mainlobe is an interesting aspect. The closer the mainlobe and the clutter signal becomes the more of a challenge it becomes for the configurations to cancel out the clutter while maximizing the mainlobe. However, when the clutter angle enter the mainlobe that is when the DPSS configuration excels. Figure 4.12 illustrates how the two configurations handles the clutter in the mainlobe. Both configurations did place a notch at the clutter direction. Although the auxiliary configuration struggled with keeping the power in the mainlobe, while the DPSS configuration succeeded pretty well.

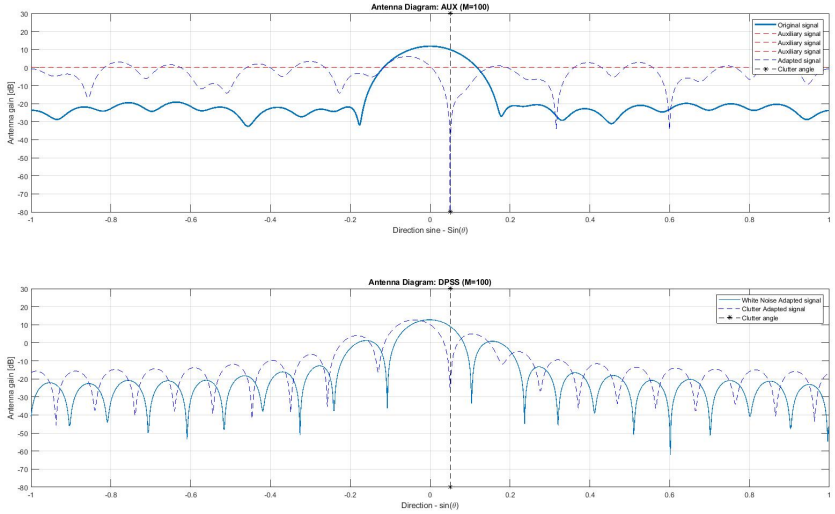

Figure 4.12: Comparison of the two configuration for the case of a single clutter signal in the mainlobe. Top plot shows the auxiliary and the botton the DPSS

The IF and SINR for this simulation is shown in figure 4.13. The IF still seems to be fine based in this figure. However, the same method for caluclations of the estimated covariance matrix was used as for the "true" covariance matrix. The only difference is the number of samples used in these calculations in an attempt to get as close to the true covariance matrix as possible. For situations of configurations limitations the true and the estimated covariance matrix may have the same performance resulting in a good ratio of them two. The SINR is still worth analysing. Note how the DPSS configuration manage to reach a stability level at 10 dB, while the auxiliary configuration stabilises around 6 dB. Simulations showed that for directions closer to the mainlobe the DPSS in general performed better than the auxiliary configuration.

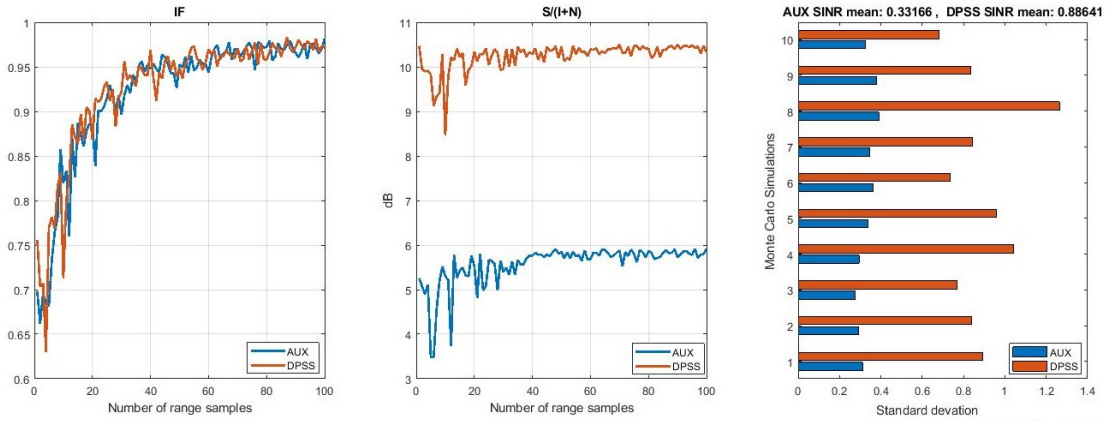

Figure 4.13: IF, SINR and standard deviation for simulation shown in figure 4.12

4.3.2 Multiple clutter signals

Four channels are used for the following simulations varying the number of clutter directions.

Two clutter signals

Both configurations performed well when exposed to two clutter signals that were far from the mainlobe, see figure 4.14 a). Just as for the single clutter signal situation, the auxiliary configuration failed to cancel out the clutter signals while maximizing the mainlobe power when the clutter entered the mainlobe. While the DPSS handles one clutter in mainlobe well. When both clutter signals enter the mainlobe the DPSS also struggles. When the clutter signals are placed close the DPSS still manage to place notches and keeping the high power in mainlobe. However, for the case that both clutter signals are in the mainlobe but not close to each other the DPSS performs poorly.

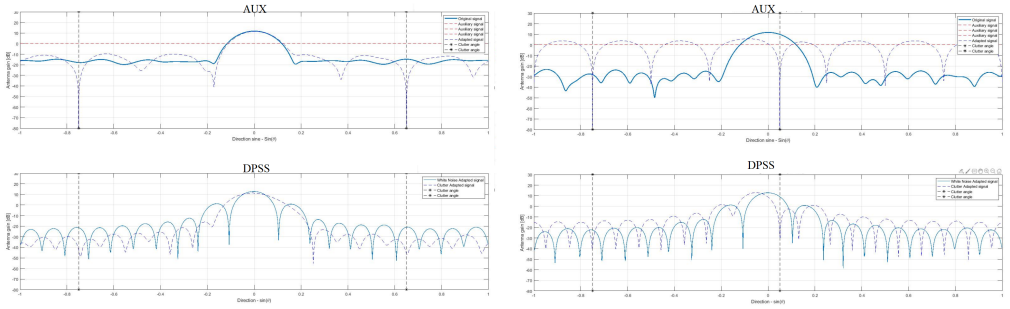

a) Two clutter signals, both far from mainlobe

b) Two clutter signals, one in mainlobe

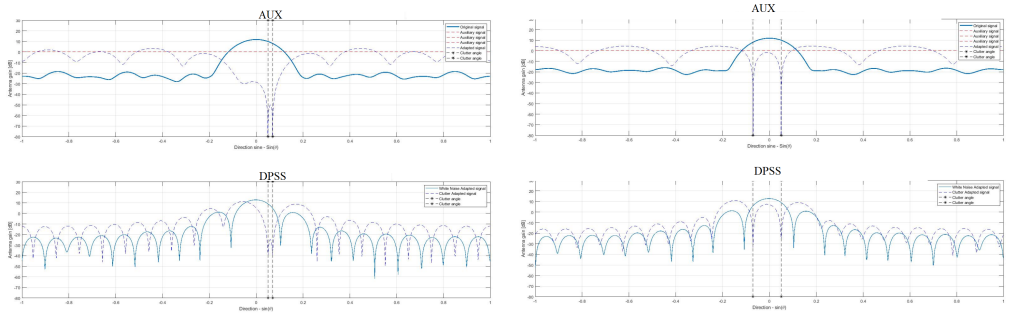

c) Two clutter signals, both in mainlobe

d) Two clutter signals, both in mainlobe

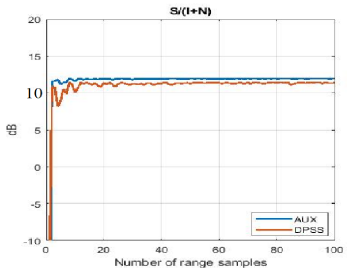

SINR of a)

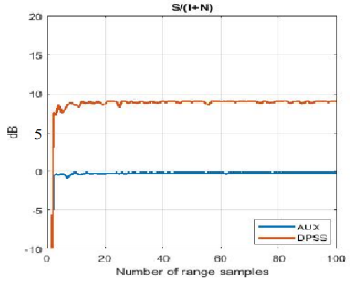

SINR of b)

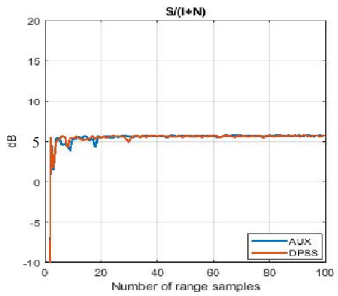

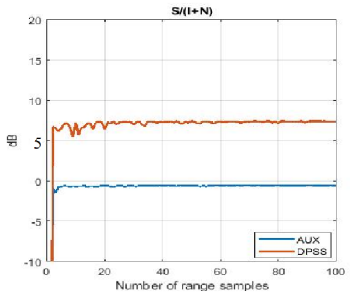

Figure 4.14: Comparison of the two configuration performances with two clutter angles to cancel out. Tested for the cases when the clutter angle are located far from mainlobe and/or in mainlobe

Three clutter signals

Note that for these simulations with four channels, three clutter signals is the same number of clutter signals as there are auxiliary channels. This could be a problem. Figure 4.15 illustrated the configurations performances for three clutter signals. The auxiliary performs often well while the clutter signals is located far from the mainlobe. Although the auxiliary fails sometimes to cancel out the clutter signals. While the DPSS handles this case well. When the clutter signals move in to the mainlobe, that is when the DPSS struggles as well.

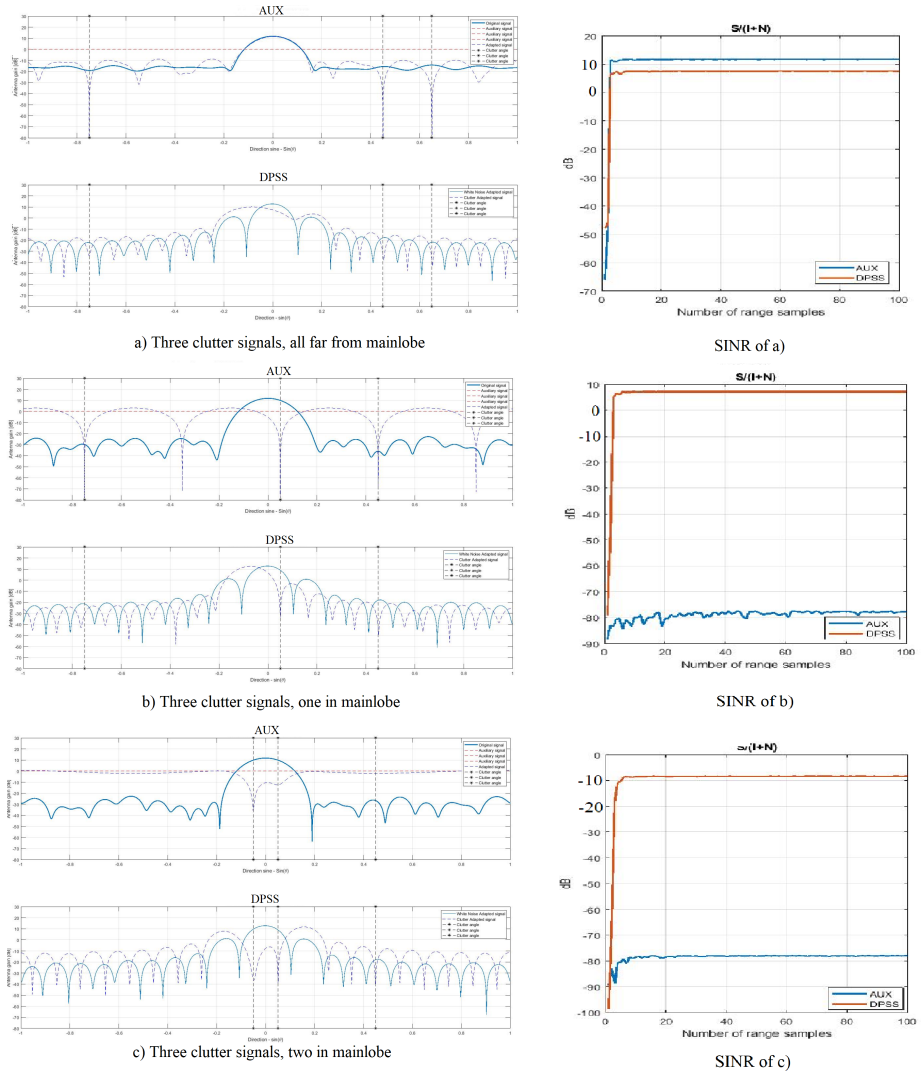

Figure 4.15: Comparison of the two configuration performances with three clutter angles to cancel out. Tested for the cases when the clutter angle are located far from mainlobe and/or in mainlobe

Four clutter signals

Note four clutter signals is the same number of clutter signals as there are channels for these simulations. Neither of the configuration performed very well. This is not unexpected. Since there are more clutter signals than there are auxiliary channels or equal the discrete prolate spheroidal sequences the weighting of the signals becomes difficult.

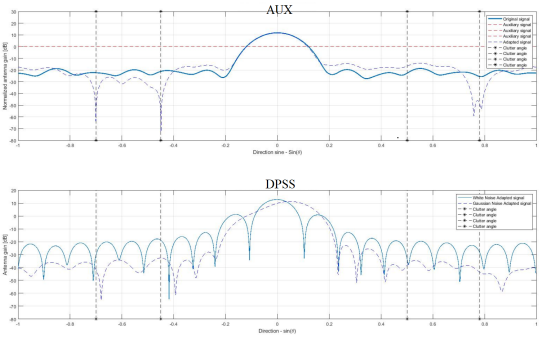

a) Four clutter signals, all far from mainlobe

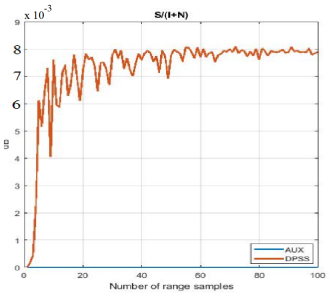

SINR of a)

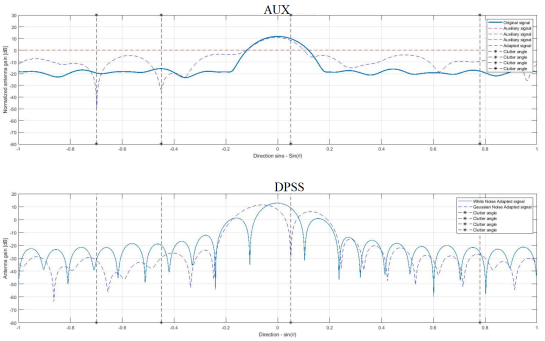

b) Four clutter signals, one in mainlobe

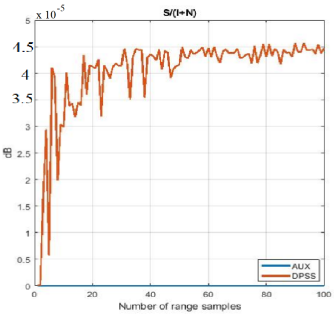

SINR of b)

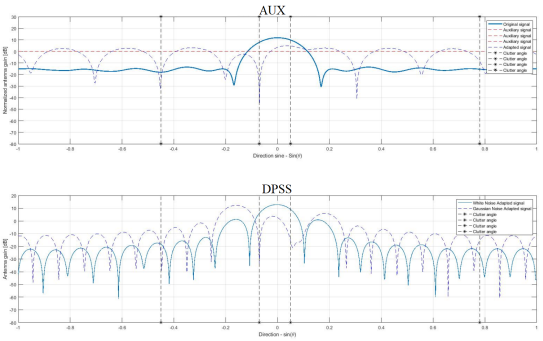

c) Four clutter signals, two in mainlobe

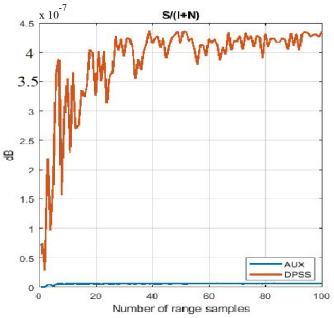

SINR of c)

Figure 4.16: Comparison of the two configuration performances with four clutter angles to cancel out. Tested for the cases when the clutter angle are located far from mainlobe and/or in mainlobe

Chapter 5

Discussion

Both configurations are valid alternatives for clutter suppression for airborne radar systems. For clutter signals in the sidelobes they both suppressed clutter successfully. Although, when the number of clutter signals approached the number of channels used in simulations they struggled. This is not surprising. Each channel contains information regarding the target and/or the clutter signal. For optimal clutter suppression one need at least one channel/clutter signal plus one more channel. The latter channel contains the information about the target. When there are the same number of clutter signals as there are channels or more, then the configurations need to use the channels in a compromising way. Which may result in a bad clutter suppression performance.

Antenna configuration 1 - Auxiliary antennas

According to the Monte Carlo simulations the auxiliary generally generated more stable results than the DPSS. There are a couple ways that the auxiliary configuration performs better than the DPSS configuration. Such as the auxiliary generated more distinct notches and could suppress clutter signals with higher power than the DPSS. However, the auxiliary struggled more in situations when the clutter signal approached the mainlobe. Which is a problem.

Antenna configuration 2 - DPSS

Based on this thesis the DPSS configurations seems to manage clutter signals close to or in the mainlobe better than the auxiliary configuration. Which could lead to conclusion that the DPSS configuration is the better choise. However, the DPSS did sometimes fail to correctly suppress the clutter signal. Even if the DPSS seldom failed, it is a factor to consider. The result indicate that the problem is related to the taperings which became useless when the FFT of the taperings where zero in the direction of both the target and the clutter. Similar to the need for at least the same number of channels as there are clutter signals. Otherwise there are just not enough information regarding the target and clutter to maximize the mainlobe while minimizing the clutters. When analysing figure 4.9 again one notice several directions where the DPSS could have problem with suppression of clutter. Every direction where the purple and the orange curve were both zeroed, were possible directions for which the DPSS may not have been able to suppress clutter. Although,

the result also indicated that the DPSS could compromise to still suppress the clutter. Again, in general the DPSS succeeded with the clutter suppression and seldom failed. However, to minimize the risk of DPSS fail one could try using more channels. Both configurations performed in general well in simulation with twice as many channels as clutter signals or more. Although remember, the more channels used the more samples is required to generate a good covariance matrix for the STAP algorithm.

The DPSS generated good enough notches in clutter directions and also manage clutter close to or in the mainlobe better than the auxiliary configuration. Which is desirable for airbore surveillance radars.

5.1 Conclusion

One conclusion of this thesis is that for both configurations the same number of training data is required for them to generate an acceptable performance, which is at lest 10 times the number of channels. Thus, when using many channels one need to consider the amount of samples neeeded.

Both configurations seems to be valid options for airborne surveillance radars. Although this thesis conclude that the DPSS configuration to be the superior option for this theses. Since this thesis focus on the performance of the configurations for when clutter angles are close to the mainlobe. The results clearly indicate that the DPSS configuration handles clutter in the mainlobe better than the auxiliary configuration. Although, one need to be aware of the problem with the DPSS occasionally failing to cancel out the clutter.

5.2 Future work

Adding clutter detection to the simulation would be a good next step for analysing these configurations. But first, analysing and finding a solution to the rare occurrence of clutter suppression fail of the DPSS configuration.

Appendix A

Derivations

A.1 Equation 2.25 - well known linear weighting

Following derivation can be found in L.E BRENNAN and L.S. REED *Theory of Adaptive Radar* paper, published in marsh of 1973.[8] Note that some of the notations(namnes,symbols) in this derivation differs from the ones used in this report.

Assume that a radar sends an electromagnetic signal. Suppose an echo from a target is received by a set of **N** sensors. Let S be the expected sensor data from the target:

$$S = \begin{pmatrix} s_1 \\ s_2 \\ \vdots \\ s_m \end{pmatrix} \tag{A.1}$$

Each sensor takes a number **K** samples, where s_k is a complex number, the sampled phase and envelope for K = 1,2, ..., n, and $n = \mathbf{NK}$ is the total number of space-time samples.

The vector S is called the signal vector. Let the following column vector be the noise vector.

$$N = \begin{pmatrix} n_1 \\ n_2 \\ \vdots \\ n_n \end{pmatrix} \tag{A.2}$$

The sum of vectors S and N is the signal-plus-noise vector:

$$Z = S + N \tag{A.3}$$

The radar problem is to detect the signal vector among the noise vectors. To find S one puts the received vectors through a "filter" with so called weights:

$$W = \begin{pmatrix} w_1 \\ w_2 \\ \vdots \\ w_n \end{pmatrix} \tag{A.4}$$

where the output of filter W is:

$$X = \sum_{k=1}^{n} w_k z_k = W^T Z \tag{A.5}$$

where T denotes matrix transpose. For noise alone is the expected value of X zero, thus:

$$EX = \sum_{k=1}^{n} w_k s_k = W^T S \tag{A.6}$$

for signal plus noise. Similarly, the noise power or variance of X is:

$$\sigma^2 = E|X|^2 - |EX|^2 = W^H \overline{EN} N^T W = W^H M W \tag{A.7}$$

where "H" denotes the hermitian transpose, $\overline{EN}$ denotes the complex conjugate of EN and M is the coveriance matrix of the noise.

$$M = \overline{EN} N^T \tag{A.8}$$

Clutter and other interference sources are approximately Gaussian. Assume the elements in vector N have complex variate with complex coveriance M. Then the output X of the filter W has the probability density:

$$P\{X|Z = N\} = \frac{1}{2\pi\sigma^2} exp\left(\frac{-|X|^2}{2\sigma^2}\right) \tag{A.9}$$

for noise alone. For signal plus noise, the probability density is:

$$P\{X|Z = S + N\} = \frac{1}{2\pi\sigma^2} exp\left(\frac{-|X - W^T S|^2}{2\sigma^2}\right) \tag{A.10}$$

A likelihood ratio test is the best decision criterion for detecting the signal S in the presence of noise N:

$$L = \frac{P\{X|Z = S + N\}}{P\{X|Z = N\}} = exp\left[\frac{1}{2\pi\sigma^2}(S_1\overline{X} + \overline{S}_1X - S_1\overline{S}_1)\right] = exp\left[\frac{1}{2\pi\sigma^2}(2|S_1||X|\cos(\theta - \delta) - |S_1|^2)\right] \tag{A.11}$$

where

$$S_1 = W^T S \tag{A.12}$$

and

$$\theta = arg(X) \tag{A.13}$$

$$\delta = arg(S_1) \tag{A.14}$$

Assume the distribution of phase θ uniformly from 0 to 2π, since the target position is usually not known with certainty. If the probability density of $P(\theta)$ is known, then the best test for detection is the optimum Bayes test. This test is formed by averanging L with respect to θ and by comparing the result with a threshold c. That is, if:

$$\int L(X|\theta)P(\theta)d\theta \geq c > 0 \tag{A.15}$$

The signal is said to be detected if this quantity is less than c. X is said to result from noise alone. Since $P(\theta) = 1/2\pi$ one gets,

$$exp\left(\frac{-|S_1|^2}{2\sigma^2}\right)\int_0^{2\phi} exp\left[|S_1||X|\cos(\theta - \delta)\right]\frac{d\theta}{2\phi} = exp\left(\frac{-|S_1|^2}{2\sigma^2}\right)I_0(|S_1||X|) \geq c \tag{A.16}$$

where I_0 is the modified zero-order Bessel function of the first kind. Since I_0 an increasing function of x and c is a positive constant, the test above can be simplified to:

$$|X| \geq k \tag{A.17}$$

where k is related to c by:

$$exp\left(\frac{-|S_1|^2}{2\sigma^2}\right)I_0(|S_1|k) = c \tag{A.18}$$

The probability of false alarm P_F and the probability of detection P_D for the simplified test are:

$$P_F = prob\{|X| > k|Z = N\} = \int_k^\infty \int_0^{2\pi} \frac{1}{2\sigma^2} exp\left(\frac{-r^2}{2\sigma^2}\right) r dr d\theta = exp\left(\frac{-k^2}{2\sigma^2}\right) \tag{A.19}$$

and

$$P_D = prob\{|X| > k|Z = S + N\} = \int_k^\infty \int_0^{2\pi} exp\left(\frac{-1}{2\sigma^2}|re^{i\theta} - ae^{i\delta}|^2\right) \frac{r dr d\theta}{2\pi\sigma^2} = \tag{A.20}$$

$$= \frac{1}{\sigma^2} \int_k^\infty I_0\left(\frac{ra}{\sigma^2}\right) exp\left(\frac{-r^2 + a^2}{2\sigma^2}\right) r dr \tag{A.21}$$

where

$$a = |S_1| = |W_T S| \tag{A.22}$$

$$\sigma^2 = W^H M W \tag{A.23}$$

The above probability of detection can be expressed in terms of the Q function defined by Marcum and Swerling as:

$$Q(\alpha, \beta) = \int_\beta^\infty v exp\left[\frac{-(v^2 + \alpha^2)}{2}\right] I_0(\alpha v) dv \tag{A.24}$$

if one makes the following substitutions:

$$v = \frac{r}{\sigma}, \quad \alpha = \frac{a}{\sigma}, \quad \beta = \frac{k}{\sigma} \tag{A.25}$$

and put in equation for P_D one gets:

$$P_D = Q(\alpha, \beta) \tag{A.26}$$

where β is the normalized threshold:

$$\beta = \frac{k}{\sigma} = \frac{k}{\sqrt{W^H M W}} \tag{A.27}$$

and α^2 is the output or integrated signal-to-noise ratio:

$$\alpha^2 = \left(\frac{S}{N}\right) = \frac{|W^T S|^2}{W^H M W} \tag{A.28}$$

Simularly, the false alarm probability becomes:

$$P_F = exp\left(\frac{-\beta^2}{2}\right) \tag{A.29}$$

in terms of normalized threshold β, which is determined from

$$\beta = \sqrt{2log\frac{1}{P_F}} \tag{A.30}$$

Knowing this one can rewrite the equation for P_D

$$P_D(\alpha) = Q\left(\alpha, \sqrt{2log\frac{1}{P_F}}\right) = \int_{\sqrt{2log\frac{1}{P_F}}}^{\infty} vexp\left(\frac{-(v^2+\alpha^2)}{2}\right) I_0(\alpha v)dv \tag{A.31}$$

in terms of signal-to-noise rato α^2 and false alarm probability P_F. Nnote that if P_F is fixed, the probability of detection is a function of only α.

The function $P_D(\alpha)$ is an increasing function of α. This can be shown by first looking at the equation for the signal-to-noise ratio α^2, note that the equation is a function of the weight vector W. So α will vary with the components of the filter W used to detect S. If $P_D(\alpha)$ can be shown to increase with α, the probability of detection will be highest for that filter W which maximizes α. First, let:

$$\frac{d}{dx}I_0(x) = I_1(x) \tag{A.32}$$

$$\frac{d}{dx}xI_1(x) = xI_0(x) \tag{A.33}$$

given by

$$\frac{d}{d\alpha}\left[P_D(\alpha)\right] = \int_{\sqrt{2log\frac{1}{P_F}}}^{\infty} exp\frac{-(v^2+\alpha^2)}{2}\left[v^2 I_1(\alpha v) - \alpha v I_0(\alpha v)\right]dv = \tag{A.34}$$

$$= \int_{\sqrt{2log\frac{1}{P_F}}}^{\infty} -dexp\left[\frac{-(v^2+\alpha^2)}{2}[vI_1(\alpha v)]\right] = \beta exp\frac{-(\beta^2+\alpha^2)}{2}I_1(\alpha\beta) \tag{A.35}$$

where

$$\beta = \sqrt{2log\frac{1}{P_F}} > 0 \tag{A.36}$$

By the fact that $I_1(x) > 0$ for all $x > 0$, one then gets

$$\frac{d}{d\alpha}P_D(\alpha) > 0 \tag{A.37}$$

for all $\alpha > 0$. Thus, $P_D(\alpha)$ is an increasing function of the output of the signal-to-noise ratio α^2- to maximaize $P_D(\alpha)$ with respect to the filter W, it is only necessary to maximize α^2. To maximize

α^2 one can use the fact that the coveriance matrix M is a hermitian matrix. Therefore there exists a unitary matrix P which diagonalizes M.

$$PMP^{-1} = \Lambda \tag{A.38}$$

where

$$\Lambda = \begin{pmatrix} \lambda_1 & 0 & \dots & 0 \\ 0 & \lambda_2 & \dots & 0 \\ \vdots & \vdots & \ddots & \vdots \\ 0 & 0 & \dots & {}_n \end{pmatrix} \tag{A.39}$$

and $\lambda_k > 0$ are the eigenvalues of M for k = 1,2, ..., n. In terms of Λ and P, the square root of the matrix M is given by:

$$M^{\sqrt{\frac{1}{2}}} = P^{-1}\Lambda^{\frac{1}{2}}P \tag{A.40}$$

where $\Lambda^{\frac{1}{2}}$ is defined as:

$$\Lambda^{\frac{1}{2}} = \begin{pmatrix} \sqrt{\lambda_1} & 0 & \dots & 0 \\ 0 & \sqrt{\lambda_2} & \dots & 0 \\ \vdots & \vdots & \ddots & \vdots \\ 0 & 0 & \dots & \sqrt{\lambda_n} \end{pmatrix} \tag{A.41}$$

The signal-to-noise ratio [2] can be bounded above in the following manner. First note that:

$$\alpha^2 = \frac{|W^T S|^2}{W^H M W} = \frac{|W^T \overline{M}^{\frac{1}{2}} \overline{M}^{-\frac{1}{2}} S|^2}{W^H M W} = \frac{\left|\sum_{j=1}^n a_j b_j\right|^2}{W^H M W} \tag{A.42}$$

where

$$\overline{M}^{-\frac{1}{2}} = (\overline{M}^{\frac{1}{2}})^{-1} \tag{A.43}$$

$$a_j = \sum_{k=1}^{n} w_k \overline{M}^{\frac{1}{2}}_{kj} \tag{A.44}$$

$$b_j = \sum_{k=1}^{n} \overline{M}^{-\frac{1}{2}}_{jk} s_k \tag{A.45}$$

But, by the Schwarz inequality one has,

$$\left|\sum_{j=1}^{n} a_j b_j\right|^2 = \sum_{j=1}^{n} |a_j|^2 \sum_{j=1}^{n} |b_j|^2 \tag{A.46}$$

Thus,

$$\left(\frac{S}{N}\right)_0 = \alpha^2 \leq \frac{\sum_{j=1}^{n}|a_j|^2 \sum_{j=1}^{n}|b_j|^2}{W^H M W} = \frac{(W^H M^{\frac{1}{2}})\overline{(W^H M^{\frac{1}{2}})}(M^{-\frac{1}{2}}\overline{S})(\overline{M}^{-\frac{1}{2}}S)}{W^H M W} = \tag{A.47}$$

$$= \frac{(W^H M W)(S^H \overline{M}^{-1} S)}{W^H M W} = S M^{-1}\overline{S} \tag{A.48}$$

The bound on α^2, shown by the equation above. can be attained if one lets

$$W = k M^{-1}\overline{S} \tag{A.49}$$

where k is a complex constant not equal to zero. This can be seen by submitting equation A.49 into equation A.33,

$$\alpha^2 = \frac{|W^T S|^2}{W^H M W} = \frac{|k|^2 |S^T M^{-1} S^H|^2}{(\overline{k} S^T M^{-1}) M (k M^{-1}\overline{S})} = S^T M^{-1}\overline{S} \tag{A.50}$$

Thus, the maximum of the output signal-to-noise raito with respect to the weight vector W, that is,

$$max_w \left(\frac{S}{N}\right)_0 = max_w \alpha^2 = S^T M^{-1}\overline{S} \tag{A.51}$$

is attained if vector W is given by equation (A.49). Thus, equation (2.25) is derived.[8] For the maximum signal-to-noise power ratio has the constant k no influence on the SNR an can be chosen arbitrarily.[6] In this report it is chosen as 1, thus the well known linear weighting becomes equation (2.25).

Bibliography

[1] S. Friberg and P. Pålson. *"Space-Time Adaptive Processing in FPGA"*, chapter Chalmers University of Technology, Department of Computer Science and Engineering, Master Thesis. 2012.

[2] R. A. Freedman H. D. Young and A. L. Ford. *"University Physics"*. 2012.

[3] The Mathworks Inc. *"Taylorwin"*.

[4] The Mathworks Inc. *dpss*. "https://se.mathworks.com/help/signal/ref/dpss.html", 2018.

[5] R.W. Schafer J. . McClellan and M.A. Yoder. *"Signal Processing First"*. 2003.

[6] R. Klemm. *"Principles of space-time adaptive processing"*. 2002.

[7] D.C. Lay. *"Linear Algebra and its applications"*. 2002.

[8] L.E.Brennan and L.S.Reed. "theory of adaptive radar". *Transactions on aerospace and electronic systems*, March 1973.

[9] M. Richards. *"Fundamentals of Radar Signal Processing"*. 2005.

[10] A. Cattani F. Ghelfi A. Maccaferri S. Montebugnoli, G. Bianchi and F. Perini. *"The medicina ira-ska engineering group, some notes on beamforming,"*. http://www.ira.inaf.it/Library/rapp-int-2004/353-04.pdf, 2004.

[11] M. Skolnik. *"Introduction to radar systems"*. 1962.

[12] G. W. Stimson. *"Introduction to airborne radar"*. 1998.

[13] V.K.Garg and Y-C.Wang. *"The Electrical Engineering Handbook"*. 2005.